Chapter 7

Enhanced Sampling Algorithms

Ayori Mitsutake, Yoshiharu Mori, and Yuko Okamoto

Abstract

In biomolecular systems (especially all-atom models) with many degrees of freedom such as proteins and nucleic acids, there exist an astronomically large number of local-minimum-energy states. Conventional simulations in the canonical ensemble are of little use, because they tend to get trapped in states of these energy local minima. Enhanced conformational sampling techniques are thus in great demand. A simulation in generalized ensemble performs a random walk in potential energy space and can overcome this difficulty. From only one simulation run, one can obtain canonical-ensemble averages of physical quantities as functions of temperature by the single-histogram and/or multiple-histogram reweighting techniques. In this article we review uses of the generalized-ensemble algorithms in biomolecular systems. Three well-known methods, namely, multicanonical algorithm, simulated tempering, and replica-exchange method, are described first. Both Monte Carlo and molecular dynamics versions of the algorithms are given. We then present various extensions of these three generalized-ensemble algorithms. The effectiveness of the methods is tested with short peptide and protein systems.

Key words: Monte Carlo, Molecular dynamics, Generalized-ensemble algorithm, Replica-exchange method, Simulated tempering, Multicanonical algorithm

1. Introduction

Conventional Monte Carlo (MC) and molecular dynamics (MD) simulations of biomolecules are greatly hampered by the multiple-minima problem. The canonical fixed-temperature simulations at low temperatures tend to get trapped in a few of a huge number of local-minimum-energy states which are separated by high energy barriers. One way to overcome this multiple-minima problem is to perform a simulated annealing (SA) simulation (1), and it has been widely used in biomolecular systems (see, e.g., Refs. (2–8) for earlier applications). The SA simulation mimics the crystal-making process, and temperature is lowered very slowly from a sufficiently high temperature to a low one during the SA simulation. The Boltzmann weight factor is dynamically changed, and so the

Luca Monticelli and Emppu Salonen (eds.), *Biomolecular Simulations: Methods and Protocols*, Methods in Molecular Biology, vol. 924, DOI 10.1007/978-1-62703-017-5_7,

thermal equilibrium is continuously broken. Hence, although the global-minimum potential energy or the value close to it may be found, accurate thermodynamic averages for fixed temperatures cannot be obtained.

A class of simulation methods, which are referred to as the *generalized-ensemble algorithms*, overcome both above difficulties, namely, the multiple-minima problem and inaccurate thermodynamic averages (for reviews see, e.g., Refs. (9–16)). In the generalized-ensemble algorithm, each state is weighted by an artificial, non-Boltzmann probability weight factor so that a random walk in potential energy space may be realized. The random walk allows the simulation to escape from any energy barrier and to sample much wider conformational space than by conventional methods. Unlike SA simulations, the weight factors are fixed during the simulations so that the eventual reach to the thermal equilibrium is guaranteed. From a single simulation run, one can obtain accurate ensemble averages as functions of temperature by the single-histogram (17, 18) and/or multiple-histogram (19, 20) reweighting techniques (an extension of the multiple-histogram method is also referred to as the *weighted histogram analysis method* (WHAM) (20)).

One of the most well-known generalized-ensemble algorithms is perhaps the *multicanonical algorithm* (MUCA) (21, 22) (for reviews see, e.g., Refs. (23, 24)). The method is also referred to as *entropic sampling* (25–27) and *adaptive umbrella sampling* (28) *of the potential energy* (29). MUCA can also be considered as a sophisticated, ideal realization of a class of algorithms called *umbrella sampling* (30). Also closely related methods are *Wang-Landau method* (31, 32), which is also referred to as *density of states Monte Carlo* (33), and *meta dynamics* (34) (see also Ref. (35)). MUCA and its generalizations have been applied to spin systems (see, e.g., Refs. (36–42)). MUCA was also introduced to the molecular simulation field (43). Since then, MUCA and its generalizations have been extensively used in many applications in protein and other biomolecular systems (44–78). Molecular dynamics version of MUCA has also been developed (29, 50, 54) (see also Refs. (50, 79) for the Langevin dynamics version). MUCA has been extended so that flat distributions in other variables instead of potential energy may be obtained (see, e.g., Refs. (37, 38, 49, 55, 57, 70, 76)). This can be considered as a special case of the multidimensional (or, multivariable) extensions of MUCA, where a multidimensional random walk in potential energy space and in other variable space is realized (see, e.g., Refs. (49, 55, 56, 72, 78)). In this article, we just present one of such methods, namely, the *multibaric-multithermal algorithm* (MUBATH) where a two-dimensional random walk in both potential energy space and volume space is realized (72–75).

While a simulation in multicanonical ensemble performs a free 1D random walk in potential energy space, that in *simulated*

tempering (ST) (80, 81) (the method is also referred to as the *method of expanded ensemble* (80)) performs a free random walk in temperature space (for a review, see, e.g., Ref. (82)). This random walk, in turn, induces a random walk in potential energy space and allows the simulation to escape from states of energy local minima. ST and its generalizations have also been applied to chemical physics field and biomolecular systems (51, 52, 83–91).

MUCA and ST are powerful, but the probability weight factors are not a priori known and have to be determined by iterations of short trial simulations. This process can be nontrivial and very tedious for complex systems with many degrees of freedom.

In the *replica-exchange method* (REM) (92–94), the difficulty of weight factor determination is greatly alleviated. (A closely related method was independently developed in Ref. (95). Similar methods in which the same equations are used but emphasis is laid on optimizations have been developed (96, 97). REM is also referred to as *multiple Markov chain method* (98) and *parallel tempering* (82). Details of literature about REM and related algorithms can be found in recent reviews (10, 15, 99).) In this method, a number of noninteracting copies (or, replicas) of the original system at different temperatures are simulated independently and simultaneously by the conventional MC or MD method. Every few steps, pairs of replicas are exchanged with a specified transition probability. The weight factor is just the product of Boltzmann factors, and so it is essentially known.

REM has already been used in many applications in protein systems (100–115). Other molecular simulation fields have also been studied by this method in various ensembles (116–120). Moreover, REM was introduced to the quantum chemistry field (121). The details of molecular dynamics algorithm for REM, which is referred to as the *replica-exchange molecular dynamics* (REMD) have been worked out in Ref. (101), and this led to a wide application of REM in the protein folding and related problems (see, e.g., Refs. (122–144)).

However, REM also has a computational difficulty: As the number of degrees of freedom of the system increases, the required number of replicas also greatly increases, whereas only a single replica is simulated in MUCA and ST. This demands a lot of computer power for complex systems. Our solution to this problem is: Use REM for the weight factor determinations of MUCA, which is much simpler than previous iterative methods of weight determinations, and then perform a long MUCA production run. The method is referred to as the *replica-exchange multicanonical algorithm* (REMUCA) (105, 109, 110). In REMUCA, a short replica-exchange simulation is performed, and the multicanonical weight factor is determined by the multiple-histogram reweighting techniques (19, 20). Another example of a combination of REM and ST is the *replica-exchange simulated tempering* (REST) (86). In REST,

a short replica-exchange simulation is performed, and the simulated tempering weight factor is determined by the multiple-histogram reweighting techniques (19, 20).

We have introduced two further extensions of REM, which we refer to as *multicanonical replica-exchange method* (MUCAREM) (105, 109, 110) (see also Refs. (133, 134)) and *simulated tempering replica-exchange method* (STREM) (87) (see also Ref. (135) for a similar idea). In MUCAREM, a replica-exchange simulation is performed with a small number of replicas each in multicanonical ensemble of different energy ranges. In STREM, on the other hand, a replica-exchange simulation is performed with a small number of replicas in "simulated tempering" ensemble of different temperature ranges.

Finally, one is naturally led to a multidimensional (or, multivariable) extension of REM, which we refer to as the *multidimensional replica-exchange method* (MREM) (103) (see also Refs. (117, 145)). (The method is also referred to as *generalized parallel sampling* (146), *Hamiltonian replica-exchange method*(108), and *Model Hopping*(147).) Some other special cases of MREM can be found in, e. g., Refs. (132, 148–153). Another special realization of MREM is *replica-exchange umbrella sampling* (REUS) (103), and it is particularly useful in free energy calculations (see also Ref. (104) for a similar idea). In this article, we just present one of such methods, namely, the REM in the isobaric-isothermal ensemble, where not only temperature values but also pressure values are exchanged in the replica-exchange processes (11, 118, 120, 128, 129). (The results of the first such application of the two-dimensional replica-exchange simulations in the isobaric-isothermal ensemble were presented in Ref. (11).)

In this article, we describe the generalized-ensemble algorithms mentioned above. Namely, we first review the three familiar methods: REM, ST, and MUCA. We then describe various extensions of these methods (103, 154–157). Examples of the results by some of these algorithms are then presented.

2. Generalized-Ensemble Algorithms

2.1. Replica-Exchange Method

Let us consider a system of N atoms of mass m_k ($k = 1, \ldots, N$) with their coordinate vectors and momentum vectors denoted by $q \equiv \{\boldsymbol{q}_1, \ldots, \boldsymbol{q}_N\}$ and $p \equiv \{\boldsymbol{p}_1, \ldots, \boldsymbol{p}_N\}$, respectively. The Hamiltonian $H(q, p)$ of the system is the sum of the kinetic energy $K(p)$ and the potential energy $E(q)$:

$$H(q, p) = K(p) + E(q), \tag{1}$$

where

$$K(p) = \sum_{k=1}^{N} \frac{\boldsymbol{p}_k{}^2}{2m_k}. \tag{2}$$

In the canonical ensemble at temperature T, each state $x \equiv (q, p)$ with the Hamiltonian $H(q, p)$ is weighted by the Boltzmann factor:

$$W_{\mathrm{B}}(x; T) = \exp(-\beta H(q, p)), \tag{3}$$

where the inverse temperature β is defined by $\beta = 1/k_{\mathrm{B}}T$ (k_{B} is the Boltzmann constant). The average kinetic energy at temperature T is then given by

$$\langle K(p)\rangle_T = \left\langle \sum_{k=1}^{N} \frac{\boldsymbol{p}_k{}^2}{2m_k} \right\rangle_T = \frac{3}{2} N k_{\mathrm{B}} T. \tag{4}$$

Because the coordinates q and momenta p are decoupled in Eq. 1, we can suppress the kinetic energy part and can write the Boltzmann factor as

$$W_{\mathrm{B}}(x; T) = W_{\mathrm{B}}(E; T) = \exp(-\beta E). \tag{5}$$

The canonical probability distribution of potential energy $P_{\mathrm{NVT}}(E; T)$ is then given by the product of the density of states $n(E)$ and the Boltzmann weight factor $W_{\mathrm{B}}(E; T)$:

$$P_{\mathrm{NVT}}(E; T) \propto n(E) W_{\mathrm{B}}(E; T). \tag{6}$$

Because $n(E)$ is a rapidly increasing function and the Boltzmann factor decreases exponentially, the canonical ensemble yields a bell-shaped distribution of potential energy which has a maximum around the average energy at temperature T. The conventional MC or MD simulations at constant temperature are expected to yield $P_{\mathrm{NVT}}(E; T)$. An MC simulation based on the Metropolis algorithm (158) is performed with the following transition probability from a state x of potential energy E to a state x' of potential energy E':

$$w(x \to x') = \min\left(1, \frac{W_{\mathrm{B}}(E'; T)}{W_{\mathrm{B}}(E; T)}\right) = \min(1, \exp(-\beta \Delta E)), \tag{7}$$

where

$$\Delta E = E' - E. \tag{8}$$

A MD simulation, on the other hand, is based on the following Newton equations of motion:

$$\dot{\boldsymbol{q}}_k = \frac{\boldsymbol{p}_k}{m_k}, \tag{9}$$

$$\dot{\boldsymbol{p}}_k = -\frac{\partial E}{\partial \boldsymbol{q}_k} = \boldsymbol{f}_k, \tag{10}$$

where $\boldsymbol{f}_k$ is the force acting on the kth atom ($k = 1, \ldots, N$). This set of equations actually yield the microcanonical ensemble, however, and we have to add a thermostat in order to obtain the canonical ensemble at temperature T. Here, we just follow Nosé's prescription (159, 160), and we have

$$\dot{\boldsymbol{q}}_k = \frac{\boldsymbol{p}_k}{m_k}, \tag{11}$$

$$\dot{\boldsymbol{p}}_k = -\frac{\partial E}{\partial \boldsymbol{q}_k} - \frac{\dot{s}}{s}\boldsymbol{p}_k = \boldsymbol{f}_k - \frac{\dot{s}}{s}\boldsymbol{p}_k, \tag{12}$$

$$\dot{s} = s\frac{P_s}{Q}, \tag{13}$$

$$\dot{P}_s = \sum_{k=1}^{N} \frac{\boldsymbol{p}_k^2}{m_k} - 3Nk_{\mathrm{B}}T = 3Nk_{\mathrm{B}}(T(t) - T), \tag{14}$$

where s is Nosé's scaling parameter, P_s is its conjugate momentum, Q is its mass, and the "instantaneous temperature" $T(t)$ is defined by

$$T(t) = \frac{1}{3Nk_{\mathrm{B}}} \sum_{k=1}^{N} \frac{\boldsymbol{p}_k(t)^2}{m_k}. \tag{15}$$

However, in practice, it is very difficult to obtain accurate canonical distributions of complex systems at low temperatures by conventional MC or MD simulation methods. This is because simulations at low temperatures tend to get trapped in one or a few of local-minimum-energy states. This difficulty is overcome by, for instance, the generalized-ensemble algorithms, which greatly enhance conformational sampling.

The *REM* is one of effective generalized-ensemble algorithms. The system for REM consists of *Mnoninteracting* copies (or, replicas) of the original system in the canonical ensemble at M different temperatures T_m ($m = 1, \ldots, M$). We arrange the replicas so that there is always exactly one replica at each temperature. Then there exists a one-to-one correspondence between replicas and temperatures; the label i ($i = 1, \ldots, M$) for replicas is a permutation of the label m ($m = 1, \ldots, M$) for temperatures, and vice versa:

$$\begin{cases} i = i(m) \equiv f(m), \\ m = m(i) \equiv f^{-1}(i), \end{cases} \tag{16}$$

where $f(m)$ is a permutation function of m and $f^{-1}(i)$ is its inverse.

Let $X = \left\{x_1^{[i(1)]}, \ldots, x_M^{[i(M)]}\right\} = \left\{x_{m(1)}^{[1]}, \ldots, x_{m(M)}^{[M]}\right\}$ stand for a "state" in this generalized ensemble. Each "substate" $x_m{}^{[i]}$ is specified by the coordinates $q^{[i]}$ and momenta $p^{[i]}$ of N atoms in replica i at temperature T_m:

$$x_m^{[i]} \equiv \left(q^{[i]}, p^{[i]}\right)_m. \tag{17}$$

Because the replicas are noninteracting, the weight factor for the state X in this generalized ensemble is given by the product of Boltzmann factors for each replica (or at each temperature):

$$\begin{aligned} W_{\mathrm{REM}}(X) &= \prod_{i=1}^{M} \exp\left\{-\beta_{m(i)} H\left(q^{[i]}, p^{[i]}\right)\right\} \\ &= \prod_{m=1}^{M} \exp\left\{-\beta_m H\left(q^{[i(m)]}, p^{[i(m)]}\right)\right\}, \\ &= \exp\left\{-\sum_{i=1}^{M} \beta_{m(i)} H\left(q^{[i]}, p^{[i]}\right)\right\} \\ &= \exp\left\{-\sum_{m=1}^{M} \beta_m H\left(q^{[i(m)]}, p^{[i(m)]}\right)\right\}, \end{aligned} \tag{18}$$

where $i(m)$ and $m(i)$ are the permutation functions in Eq. 16.

We now consider exchanging a pair of replicas in this ensemble. Suppose we exchange replicas i and j which are at temperatures T_m and T_n, respectively:

$$X = \left\{\ldots, x_m^{[i]}, \ldots, x_n^{[j]}, \ldots\right\} \to X' = \left\{\ldots, x_m^{[j]\prime}, \ldots, x_n^{[i]\prime}, \ldots\right\}. \tag{19}$$

Here, i, j, m, and n are related by the permutation functions in Eq. 16, and the exchange of replicas introduces a new permutation function f':

$$\begin{cases} i = f(m) \to j = f'(m), \\ j = f(n) \to i = f'(n)\cdot \end{cases} \tag{20}$$

The exchange of replicas can be written in more detail as

$$\begin{cases} x_m^{[i]} \equiv \left(q^{[i]}, p^{[i]}\right)_m \to x_m^{[j]\prime} \equiv \left(q^{[j]}, p^{[j]\prime}\right)_m, \\ x_n^{[j]} \equiv \left(q^{[j]}, p^{[j]}\right)_n \to x_n^{[i]\prime} \equiv \left(q^{[i]}, p^{[i]\prime}\right)_n, \end{cases} \tag{21}$$

where the definitions for $p^{[i]'}$ and $p^{[j]'}$ will be given below. We remark that this process is equivalent to exchanging a pair of temperatures T_m and T_n for the corresponding replicas i and j as follows:

$$\begin{cases} x_m^{[i]} \equiv \left(q^{[i]}, p^{[i]}\right)_m \to x_n^{[i]\prime} \equiv \left(q^{[i]}, p^{[i]\prime}\right)_n, \\ x_n^{[j]} \equiv \left(q^{[j]}, p^{[j]}\right)_n \to x_m^{[j]\prime} \equiv \left(q^{[j]}, p^{[j]\prime}\right)_m. \end{cases} \tag{22}$$

In the original implementation of the *REM* (92–94), Monte Carlo algorithm was used, and only the coordinates q (and the

potential energy function $E(q)$) had to be taken into account. In molecular dynamics algorithm, on the other hand, we also have to deal with the momenta p. We proposed the following momentum assignment in Eq. 21 (and in Eq. 22) (101):

$$\begin{cases} p^{[i]\prime} \equiv \sqrt{\frac{T_n}{T_m}}\, p^{[i]}, \\ p^{[j]\prime} \equiv \sqrt{\frac{T_m}{T_n}}\, p^{[j]}, \end{cases} \tag{23}$$

which we believe is the simplest and the most natural. This assignment means that we just rescale uniformly the velocities of all the atoms in the replicas by the square root of the ratio of the two temperatures so that the temperature condition in Eq. 4 may be satisfied immediately after replica exchange is accepted.

The transition probability of this replica-exchange process is given by the usual Metropolis criterion:

$$w(X \to X') \equiv w\left(x_m^{[i]} \mid x_n^{[j]}\right) = \min\left(1, \frac{W_{\mathrm{REM}}(X')}{W_{\mathrm{REM}}(X)}\right) = \min(1, \exp(-\Delta)), \tag{24}$$

where in the second expression (i.e., $w(x_m{}^{[i]}|x_n{}^{[j]})$) we explicitly wrote the pair of replicas (and temperatures) to be exchanged. From Eqs. 1, 2, 18, and 23, we have

$$\begin{aligned} &\frac{W_{\mathrm{REM}}(X')}{W_{\mathrm{REM}}(X)} \\ &= \exp\Big\{-\beta_m\Big[K\left(p^{[j]\prime}\right) + E\left(q^{[j]}\right)\Big] - \beta_n\Big[K\left(p^{[i]\prime}\right) + E\left(q^{[i]}\right)\Big] \\ &\quad +\beta_m\Big[K\left(p^{[i]}\right) + E\left(q^{[i]}\right)\Big] + \beta_n\Big[K\left(p^{[j]}\right) + E\left(q^{[j]}\right)\Big]\Big\}, \\ &= \exp\Big\{-\beta_m \frac{T_m}{T_n} K\left(p^{[j]}\right) - \beta_n \frac{T_n}{T_m} K\left(p^{[i]}\right) + \beta_m K\left(p^{[i]}\right) + \beta_n K\left(p^{[j]}\right) \\ &\quad -\beta_m\Big[E\left(q^{[j]}\right) - E\left(q^{[i]}\right)\Big] - \beta_n\Big[E\left(q^{[i]}\right) - E\left(q^{[j]}\right)\Big]\Big\}. \end{aligned} \tag{25}$$

Because the kinetic energy terms in this equation all cancel out, Δ in Eq. 24 becomes

$$\Delta = \beta_m\left(E\left(q^{[j]}\right) - E\left(q^{[i]}\right)\right) - \beta_n\left(E\left(q^{[j]}\right) - E\left(q^{[i]}\right)\right), \tag{26}$$

$$= (\beta_m - \beta_n)\left(E\left(q^{[j]}\right) - E\left(q^{[i]}\right)\right). \tag{27}$$

Here, i, j, m, and n are related by the permutation functions in Eq. 16 before the replica exchange:

$$\begin{cases} i = f(m), \\ j = f(n). \end{cases} \tag{28}$$

Note that after introducing the momentum rescaling in Eq. 23, we have the same Metropolis criterion for replica exchanges, i.e., Eqs. 24 and 27, for both MC and MD versions.

Without loss of generality, we can assume $T_1 < T_2 < \cdots < T_M$. The lowest temperature T_1 should be sufficiently low so that the simulation can explore the global-minimum-energy region, and the highest temperature T_M should be sufficiently high so that no trapping in an energy-local-minimum state occurs. A simulation of the *REM* is then realized by alternately performing the following two steps:

1. Each replica in canonical ensemble of the fixed temperature is simulated *simultaneously* and *independently* for a certain MC or MD steps.
2. A pair of replicas at neighboring temperatures, say $x_m^{[i]}$ and $x_{m+1}^{[j]}$, are exchanged with the probability $w(x_m^{[i]}|x_{m+1}^{[j]})$ in Eq. 24.

Note that in Step 2 we exchange only pairs of replicas corresponding to neighboring temperatures, because the acceptance ratio of the exchange process decreases exponentially with the difference of the two β's (see Eqs. 27 and 24). Note also that whenever a replica exchange is accepted in Step 2, the permutation functions in Eq. 16 are updated. A random walk in "temperature space" is realized for each replica, which in turn induces a random walk in potential energy space. This alleviates the problem of getting trapped in states of energy local minima.

The REM simulation is particularly suitable for parallel computers. Because one can minimize the amount of information exchanged among nodes, it is best to assign each replica to each node (exchanging pairs of temperature values among nodes is much faster than exchanging coordinates and momenta). This means that we keep track of the permutation function $m(i;t) = f^{-1}(i;t)$ in Eq. 16 as a function of MC or MD step t during the simulation. After parallel canonical MC or MD simulations for a certain steps (Step 1), $M/2$ pairs of replicas corresponding to neighboring temperatures are simultaneously exchanged (Step 2), and the pairing is alternated between the two possible choices, i.e., (T_1, T_2), (T_3, T_4), ... and (T_2, T_3), (T_4, T_5), ...

After a long production run of a replica-exchange simulation, the canonical expectation value of a physical quantity A at temperature T_m ($m = 1, \ldots, M$) can be calculated by the usual arithmetic mean:

$$<A>_{T_m} = \frac{1}{n_m} \sum_{k=1}^{n_m} A(x_m(k)), \tag{29}$$

where $x_m(k)$ $(k = 1, \ldots, n_m)$ are the configurations obtained at temperature T_m and n_m is the total number of measurements made at $T = T_m$. The expectation value at any intermediate temperature $T(= 1/k_B\beta)$ can also be obtained as follows:

$$<A>_T = \frac{\sum_E A(E) P_{\mathrm{NVT}}(E; T)}{\sum_E P_{\mathrm{NVT}}(E; T)} = \frac{\sum_E A(E) n(E) \exp(-\beta E)}{\sum_E n(E) \exp(-\beta E)}. \quad (30)$$

The summation instead of integration is used in Eq. 30, because we often discretize the potential energy E with step size $\epsilon (E = E_i; i = 1, 2, \ldots)$. Here, the explicit form of the physical quantity A should be known as a function of potential energy E. For instance, $A(E) = E$ gives the average potential energy $<E>_T$ as a function of temperature, and $A(E) = \beta^2 (E - <E>_T)^2$ gives specific heat.

The density of states $n(E)$ in Eq. 30 is given by the multiple-histogram reweighting techniques (19, 20) as follows. Let $N_m(E)$ and n_m be respectively the potential-energy histogram and the total number of samples obtained at temperature $T_m = 1/k_B\beta_m$ $(m = 1, \ldots, M)$. The best estimate of the density of states is then given by (19, 20)

$$n(E) = \frac{\sum_{m=1}^{M} g_m^{-1} N_m(E)}{\sum_{m=1}^{M} g_m^{-1} n_m \exp(f_m - \beta_m E)}, \quad (31)$$

where we have for each m $(= 1, \ldots, M)$

$$\exp(-f_m) = \sum_E n(E) \exp(-\beta_m E). \quad (32)$$

Here, $g_m = 1 + 2\tau_m$, and τ_m is the integrated autocorrelation time at temperature T_m. For many systems, the quantity g_m can safely be set to be a constant in the reweighting formulae (20), and hereafter we set $g_m = 1$.

Note that Eqs. 31 and 32 are solved self-consistently by iteration (19, 20) to obtain the density of states $n(E)$ and the dimensionless Helmholtz free energy f_m. Namely, we can set all the f_m $(m = 1, \ldots, M)$ to, e.g., zero initially. We then use Eq. 31 to obtain $n(E)$, which is substituted into Eq. 32 to obtain next values of f_m, and so on.

Moreover, the ensemble averages of any physical quantity A (including those that cannot be expressed as functions of potential energy) at any temperature $T(= 1/k_B\beta)$ can now be obtained from the "trajectory" of configurations of the production run. Namely, we first obtain f_m $(m = 1, \ldots, M)$ by solving Eqs. 31 and 32 self-consistently, and then we have (109) (see also (161))

$$<A>_T = \frac{\sum_{m=1}^{M}\sum_{k=1}^{n_m} A(x_m(k)) \frac{1}{\sum_{\ell=1}^{M} n_\ell \exp\left[f_\ell - \beta_\ell E(x_m(k))\right]} \exp[-\beta E(x_m(k))]}{\sum_{m=1}^{M}\sum_{k=1}^{n_m} \frac{1}{\sum_{\ell=1}^{M} n_\ell \exp\left[f_\ell - \beta_\ell E(x_m(k))\right]} \exp[-\beta E(x_m(k))]}, \tag{33}$$

where $x_m(k)$ $(k = 1, \ldots, n_m)$ are the configurations obtained at temperature T_m.

Eqs. 30 and 31 or any other equations which involve summations of exponential functions often encounter with numerical difficulties such as overflows. These can be overcome by using, for instance, the following equation (23, 162): For $C = A + B$ (with $A > 0$ and $B > 0$), we have

$$\begin{aligned} \ln C &= \ln\left[\max(A, B)\left(1 + \frac{\min(A, B)}{\max(A, B)}\right)\right], \\ &= \max(\ln A, \ln B) + \ln\{1 + \exp[\min(\ln A, \ln B) - \max(\ln A, \ln B)]\}. \end{aligned} \tag{34}$$

We now give more details about the momentum rescaling in Eq. 23 (163). Actually, Eq. 23 is only valid for the Langevin dynamics (164), Andersen thermostat (165), and Gaussian constraint method (166–168). The former two thermostats are based on the weight factor of Eq. 3 with Eqs. 1 and 2, and the Gaussian constraint method is based on the following weight factor:

$$W(q, p) = \delta\left(\sum_{k=1}^{N} \frac{\boldsymbol{p}_k^2}{2m_k} - \frac{g k_B T}{2}\right) \exp[-\beta E(q)]. \tag{35}$$

For Nosé's method (159, 160), which gives the equations of motion in Eqs. 11–14, the Nosé Hamiltonian is given by

$$H_{\text{Nose}} = \sum_{k=1}^{N} \frac{\tilde{\boldsymbol{p}}_k^2}{2m_k s^2} + E(q) + \frac{P_s^2}{2Q} + g k_B T \log s. \tag{36}$$

Here, $g\,(=3N)$ is the number of degrees of freedom, s is a position variable of the thermostat, P_s is a momentum conjugate to s, and $\tilde{\boldsymbol{p}}_k$ is a virtual momentum, which is related to the real momenta $\boldsymbol{p}_k$ as $\boldsymbol{p}_k = \tilde{\boldsymbol{p}}_k / s$. The weight factor for the Nosé's method is then given by

$$W(q, \tilde{p}, s, P_s) = \delta(H_{\text{Nose}} - \mathcal{E}), \tag{37}$$

where $\mathcal{E}$ is the initial value of H_{Nose}. Namely, in the Nosé's method, the entire system including the thermostat is in the microcanonical ensemble. Note that the mass Q of the thermostat can have different values in each replica in REMD simulations. The rescaling method for the Nosé thermostat is given by Eq. 23 and

$$P_s^{[i]\prime} = \sqrt{\frac{T_n Q_n}{T_m Q_m}} P_s^{[i]}, \quad P_s^{[j]\prime} = \sqrt{\frac{T_m Q_m}{T_n Q_n}} P_s^{[j]}, \tag{38}$$

$$s^{[i]\prime} = s^{[i]} \exp\left[\frac{1}{g k_{\mathrm{B}}}\left(\frac{E(q^{[i]}) - \mathcal{E}_m}{T_m} - \frac{E(q^{[i]}) - \mathcal{E}_n}{T_n}\right)\right],$$

$$s^{[j]\prime} = s^{[j]} \exp\left[\frac{1}{g k_{\mathrm{B}}}\left(\frac{E(q^{[j]}) - \mathcal{E}_n}{T_n} - \frac{E(q^{[j]}) - \mathcal{E}_m}{T_m}\right)\right], \tag{39}$$

where $\mathcal{E}_m$ and $\mathcal{E}_n$ are the initial values of H_{Nose} in the simulations with T_m and T_n, respectively, before the replica exchange. Note that the real momenta have to be used in the rescaling method in Eq. 23, not the virtual momenta.

For the Nosé–Hoover thermostat (169), the states are specified by the following weight factor:

$$W(q, p, \zeta) = \exp\left[-\beta\left(\sum_{k=1}^{N} \frac{\boldsymbol{p}_k^2}{2m_k} + E(q) + \frac{Q}{2}\zeta^2\right)\right], \tag{40}$$

where ζ is a velocity of the thermostat and Q is its mass parameter. The rescaling method for the Nosé–Hoover thermostat is given by Eq. 23 and

$$\zeta^{[i]\prime} = \sqrt{\frac{T_n Q_m}{T_m Q_n}} \zeta^{[i]}, \quad \zeta^{[j]\prime} = \sqrt{\frac{T_m Q_n}{T_n Q_m}} \zeta^{[j]}, \tag{41}$$

where Q_m and Q_n are the mass parameters in the replicas at temperature values T_m and T_n, respectively, before the replica exchange.

The rescaling method for the Nosé–Hoover thermostat can be generalized to the Nosé–Hoover chains (170) in a similar way. The weight factor for the Nosé–Hoover chains is given by

$$W(q, p, \zeta_1, \ldots, \zeta_{\mathcal{L}}) = \exp\left[-\beta\left(\sum_{k=1}^{N} \frac{\boldsymbol{p}_k^2}{2m_k} + E(q) + \sum_{\ell=1}^{\mathcal{L}} \frac{Q_\ell}{2}\zeta_\ell^2\right)\right], \tag{42}$$

where $\mathcal{L}$ is the number of thermostats, ζ_ℓ $(\ell = 1, \ldots, \mathcal{L})$ is the velocity of the ℓth thermostat, and Q_ℓ $(\ell = 1, \ldots, \mathcal{L})$ is a mass parameter corresponding to the ℓth thermostat. A rescaling method for REMD with the Nosé–Hoover chains is given by Eq. 23 and the following:

$$\zeta_\ell^{[i]\prime} = \sqrt{\frac{T_n Q_{m,\ell}}{T_m Q_{n,\ell}}} \zeta_\ell^{[i]}, \quad \zeta_\ell^{[j]\prime} = \sqrt{\frac{T_m Q_{n,\ell}}{T_n Q_{m,\ell}}} \zeta_\ell^{[j]}, \ (\ell = 1, \ldots, \mathcal{L}), \tag{43}$$

where $Q_{m,\ell}$ and $Q_{n,\ell}$ are the mass parameters in the replicas at temperature values T_m and T_n, respectively, which correspond to the ℓth thermostat.

In the Nosé-Poincaré thermostat (171), the states are specified by $x \equiv (q, \tilde{p}, s, P_s)$, and the weight factor is given by

$$W(q, \tilde{p}, s, P_s) \propto \delta[s(H_{\text{Nose}} - \mathcal{E})], \tag{44}$$

where H_{Nose} is the Nosé Hamiltonian in Eq. 36 and $\mathcal{E}$ is its initial value. A rescaling method of the Nosé-Poincaré thermostat is the same as in the Nosé's thermostat and given by Eqs. 23, 38, and 39 above.

2.2. Simulated Tempering

We now introduce another generalized-ensemble algorithm, the *simulated tempering* (ST) method (80, 81). In this method temperature itself becomes a dynamical variable, and both the configuration and the temperature are updated during the simulation with a weight:

$$W_{\text{ST}}(E; T) = \exp(-\beta E + a(T)), \tag{45}$$

where the function $a(T)$ is chosen so that the probability distribution of temperature is flat:

$$\begin{aligned} P_{\text{ST}}(T) &= \int dE\ n(E)\ W_{\text{ST}}(E; T) \\ &= \int dE\ n(E)\ \exp(-\beta E + a(T)) = \text{constant}. \end{aligned} \tag{46}$$

Hence, in simulated tempering, *temperature* is sampled uniformly. A free random walk in temperature space is realized, which in turn induces a random walk in potential energy space and allows the simulation to escape from states of energy local minima.

In the numerical work we discretize the temperature in M different values, T_m ($m = 1, \ldots, M$). Without loss of generality we can order the temperature so that $T_1 < T_2 < \cdots < T_M$. The probability weight factor in Eq. 45 is now written as

$$W_{\text{ST}}(E; T_m) = \exp(-\beta_m E + a_m), \tag{47}$$

where $a_m = a(T_m)$ ($m = 1, \ldots, M$). Note that from Eqs. 46 and 47, we have

$$\exp(-a_m) \propto \int dE\ n(E)\ \exp(-\beta_m E). \tag{48}$$

The parameters a_m are therefore "dimensionless" Helmholtz free energy at temperature T_m (i.e., the inverse temperature β_m multiplied by the Helmholtz free energy).

Once the parameters a_m are determined and the initial configuration and the initial temperature T_m are chosen, a simulated tempering simulation is realized by alternately performing the following two steps (80, 81):

1. A canonical MC or MD simulation at the fixed temperature T_m is carried out for a certain steps.

2. The temperature T_m is updated to the neighboring values $T_m \pm 1$ with the configuration fixed. The transition probability of this temperature-updating process is given by the following Metropolis criterion (see Eq. 47):

$$w(T_m \to T_{m\pm1}) = \min\left(1, \frac{W_{\mathrm{ST}}(E; T_{m\pm1})}{W_{\mathrm{ST}}(E; T_m)}\right) = \min(1, \exp(-\Delta)), \tag{49}$$

where

$$\Delta = (\beta_{m\pm1} - \beta_m)E - (\alpha_{m\pm1} - \alpha_m). \tag{50}$$

Note that in Step 2 we update the temperature only to the neighboring temperatures in order to secure sufficiently large acceptance ratio of temperature updates.

We remark that when MD simulations are performed in Step 1 above, we also have to deal with the momenta p, and the kinetic energy term should be included in the weight factor. When temperature $T_{m_0\pm1}$ is accepted for T-update in Step 2, we rescale the momenta in the same way as in REMD (101, 155, 157):

$$\boldsymbol{p}_k' = \sqrt{\frac{T_{m_0\pm1}}{T_{m_0}}}\,\boldsymbol{p}_k. \tag{51}$$

The kinetic energy terms then cancel out in Eq. 50, and we can use the same Δ in the Metropolis criterion in Step 2 for both MC and MD simulations. Similar momentum scaling formulae given above should also be introduced for various other thermostats (163).

The simulated tempering parameters $\alpha_m = \alpha(T_m)\,(m = 1, \ldots, M)$ can be determined by iterations of short trial simulations (see, e.g., Refs. (52, 82, 84) for details). This process can be nontrivial and very tedious for complex systems.

After the optimal simulated tempering weight factor is determined, one performs a long simulated tempering run once. The canonical expectation value of a physical quantity A at temperature $T_m\,(m = 1, \ldots, M)$ can be calculated by the usual arithmetic mean from Eq. 29. The expectation value at any intermediate temperature can also be obtained from Eq. 30, where the density of states is given by the multiple-histogram reweighting techniques (19, 20). Namely, let $N_m(E)$ and n_m be respectively the potential-energy histogram and the total number of samples obtained at temperature $T_m = 1/k_{\mathrm{B}}\beta_m\,(m = 1, \ldots, M)$. The best estimate of the density of states is then given by solving Eqs. 31 and 32 self-consistently.

Moreover, the ensemble averages of any physical quantity A (including those that cannot be expressed as functions of potential energy) at any temperature $T(= 1/k_{\mathrm{B}}\beta)$ can now be obtained from Eq. 33.

2.3. Multicanonical Algorithm

The third generalized-ensemble algorithm that we present is the *MUCA* (21, 22). In the multicanonical ensemble, each state is weighted by a non-Boltzmann weight factor $W_{\mathrm{MUCA}}(E)$ (which we refer to as the *multicanonical weight factor*) so that a uniform potential energy distribution $P_{\mathrm{MUCA}}(E)$ is obtained:

$$P_{\mathrm{MUCA}}(E) \propto n(E)\, W_{\mathrm{MUCA}}(E) \equiv \text{constant}. \tag{52}$$

The flat distribution implies that a free one-dimensional random walk in the potential energy space is realized in this ensemble. This allows the simulation to escape from any local-minimum-energy states and to sample the configurational space much more widely than the conventional canonical MC or MD methods.

The definition in Eq. 52 implies that the multicanonical weight factor is inversely proportional to the density of states, and we can write it as follows:

$$W_{\mathrm{MUCA}}(E) \equiv \exp[-\beta_a E_{\mathrm{MUCA}}(E; T_a)] = \frac{1}{n(E)}, \tag{53}$$

where we have chosen an arbitrary reference temperature, $T_a = 1/k_{\mathrm{B}}\beta_a$, and the "multicanonical potential energy" is defined by

$$E_{\mathrm{MUCA}}(E; T_a) \equiv k_{\mathrm{B}} T_a \ln n(E) = T_a S(E). \tag{54}$$

Here, $S(E)$ is the entropy in the microcanonical ensemble. Because the density of states of the system is usually unknown, the multicanonical weight factor has to be determined numerically by iterations of short preliminary runs (21, 22).

A multicanonical MC simulation is performed, for instance, with the usual Metropolis criterion (158): The transition probability of state x with potential energy E to state x' with potential energy E' is given by

$$\begin{aligned} w(x \to x') &= \min\left(1, \frac{W_{\mathrm{MUCA}}(E')}{W_{\mathrm{MUCA}}(E)}\right) = \min\left(1, \frac{n(E)}{n(E')}\right) \\ &= \min(1, \exp(-\beta_a \Delta E_{\mathrm{MUCA}})), \end{aligned} \tag{55}$$

where

$$\Delta E_{\mathrm{MUCA}} = E_{\mathrm{MUCA}}(E'; T_a) - E_{\mathrm{MUCA}}(E; T_a). \tag{56}$$

The MD algorithm in the multicanonical ensemble also naturally follows from Eq. 53, in which the regular constant temperature MD simulation (with $T = T_a$) is performed by replacing E by E_{MUCA} in Eq. 12 (50, 54):

$$\begin{aligned} \dot{\boldsymbol{p}}_k &= -\frac{\partial E_{\mathrm{MUCA}}(E; T_a)}{\partial \boldsymbol{q}_k} - \frac{\dot{s}}{s}\boldsymbol{p}_k \\ &= \frac{\partial E_{\mathrm{MUCA}}(E; T_a)}{\partial E}\boldsymbol{f}_k - \frac{\dot{s}}{s}\boldsymbol{p}_k. \end{aligned} \tag{57}$$

If the exact multicanonical weight factor $W_{\mathrm{MUCA}}(E)$ is known, one can calculate the ensemble averages of any physical quantity A at any temperature $T(=1/k_{\mathrm{B}}\beta)$ from Eq. 30, where the density of states is given by (see Eq. 53)

$$n(E) = \frac{1}{W_{\mathrm{MUCA}}(E)}. \tag{58}$$

In general, the multicanonical weight factor $W_{\mathrm{MUCA}}(E)$, or the density of states $n(E)$, is not *a priori* known, and one needs its estimator for a numerical simulation. This estimator is usually obtained from iterations of short trial multicanonical simulations. The details of this process are described, for instance, in Refs. (36, 45). However, the iterative process can be nontrivial and very tedious for complex systems.

In practice, it is impossible to obtain the ideal multicanonical weight factor with completely uniform potential energy distribution. The question is when to stop the iteration for the weight factor determination. Our criterion for a satisfactory weight factor is that as long as we do get a random walk in potential energy space, the probability distribution $P_{\mathrm{MUCA}}(E)$ does not have to be completely flat with a tolerance of, say, an order of magnitude deviation. In such a case, we usually perform with this weight factor a multicanonical simulation with high statistics (production run) in order to get even better estimate of the density of states. Let $N_{\mathrm{MUCA}}(E)$ be the histogram of potential energy distribution $P_{\mathrm{MUCA}}(E)$ obtained by this production run. The best estimate of the density of states can then be given by the single-histogram reweighting techniques (17, 18) as follows (see the proportionality relation in Eq. 52):

$$n(E) = \frac{N_{\mathrm{MUCA}}(E)}{W_{\mathrm{MUCA}}(E)}. \tag{59}$$

By substituting this quantity into Eq. 30, one can calculate ensemble averages of physical quantity $A(E)$ as a function of temperature. Moreover, the ensemble averages of any physical quantity A (including those that cannot be expressed as functions of potential energy) at any temperature $T(=1/k_{\mathrm{B}}\beta)$ can also be obtained as long as one stores the "trajectory" of configurations from the production run. Namely, we have (109)

$$<A>_T = \frac{\sum_{k=1}^{n_s} A(x_k)\, W_{\mathrm{MUCA}}^{-1}(E(x_k)) \exp[-\beta E(x_k)]}{\sum_{k=1}^{n_s} W_{\mathrm{MUCA}}^{-1}(E(x_k)) \exp[-\beta E(x_k)]}, \tag{60}$$

where x_k is the configuration at the kth MC (or MD) step and n_s is the total number of configurations stored. Note that when A is a function of E, Eq. 60 reduces to Eq. 30 where the density of states is given by Eq. 59.

Some remarks are in order. The major advantage of REM over other generalized-ensemble methods such as simulated tempering (80, 81) and MUCA (21, 22) lies in the fact that the weight factor is a priori known (see Eq. 18), while in simulated tempering and MUCA, the determination of the weight factors can be very tedious and time-consuming. In REM, however, the number of required replicas increases greatly ($\propto \sqrt{N}$) as the system size N increases (92), while only one replica is used in simulated tempering and MUCA. This demands a lot of computer power for complex systems. Moreover, so long as optimal weight factors can be obtained, simulated tempering and MUCA are more efficient in sampling than the REM (15, 77, 87, 110).

2.4. Replica-Exchange Simulated Tempering and Replica-Exchange Multicanonical Algorithm

The *REST* (86) and the *REMUCA* (105, 109, 110) overcome both the difficulties of ST and MUCA (the weight factor determinations are nontrivial) and REM (many replicas, or a lot of computation time, are required).

In REST (86), we first perform a short REM simulation (with M replicas) to determine the simulated tempering weight factor and then perform with this weight factor a regular ST simulation with high statistics. The first step is accomplished by the multiple-histogram reweighting techniques (19, 20), which give the dimensionless Helmholtz free energy. Let $N_m(E)$ and n_m be respectively the potential-energy histogram and the total number of samples obtained at temperature T_m ($= 1/k_B\beta_m$) of the REM run. The dimensionless Helmholtz free energy f_m is then given by solving Eqs. 31 and 32 self-consistently by iteration.

Once the estimate of the dimensionless Helmholtz free energy f_m are obtained, the simulated tempering weight factor can be directly determined by using Eq. 47 where we set $a_m = f_m$ (compare Eq. (48) with Eq. 32). A long simulated tempering run is then performed with this weight factor. Let $N_m(E)$ and n_m be respectively the potential-energy histogram and the total number of samples obtained at temperature T_m ($= 1/k_B\beta_m$) from this simulated tempering run. The multiple-histogram reweighting techniques of Eqs. 31 and 32 can be used again to obtain the best estimate of the density of states $n(E)$. The expectation value of a physical quantity A at any temperature T ($= 1/k_B\beta$) is then calculated from Eq. 30.

We now present the *REMUCA* (105, 109, 110). In REMUCA, just as in REST, we first perform a short REM simulation (with M replicas) to determine the multicanonical weight factor and then perform with this weight factor a regular multicanonical simulation with high statistics. The first step is accomplished by the multiple-histogram reweighting techniques (19, 20), which give the density of states. Let $N_m(E)$ and n_m be respectively the potential-energy histogram and the total number of samples

obtained at temperature T_m ($= 1/k_B\beta_m$) of the REM run. The density of states $n(E)$ is then given by solving Eqs. 31 and 32 self-consistently by iteration.

Once the estimate of the density of states is obtained, the multicanonical weight factor can be directly determined from Eq. 53 (see also Eq. 54). Actually, the density of states $n(E)$ and the multicanonical potential energy, $E_{\mathrm{MUCA}}(E; T_0)$, thus determined are only reliable in the following range:

$$E_1 \leq E \leq E_M, \tag{61}$$

where

$$\begin{cases} E_1 = <E>_{T_1}, \\ E_M = <E>_{T_M}, \end{cases} \tag{62}$$

and T_1 and T_M are respectively the lowest and the highest temperatures used in the REM run. Outside this range, we extrapolate the multicanonical potential energy linearly (105):

$$\mathcal{E}_{\mathrm{MUCA}}(E) \equiv$$

$$\begin{cases} \left.\dfrac{\partial E_{\mathrm{MUCA}}(E; T_0)}{\partial E}\right|_{E=E_1} (E - E_1) + E_{\mathrm{MUCA}}(E_1; T_0), & \text{for } E<E_1, \\ E_{\mathrm{MUCA}}(E; T_0), & \text{for } E_1 \leq E \leq E_M, \\ \left.\dfrac{\partial E_{\mathrm{MUCA}}(E; T_0)}{\partial E}\right|_{E=E_M} (E - E_M) + E_{\mathrm{MUCA}}(E_M; T_0), & \text{for} E>E_M. \end{cases} \tag{63}$$

For Monte Carlo method, the weight factor for REMUCA is given by substituting Eq. 63 into Eq. 53 (105, 109):

$$\begin{aligned} W_{\mathrm{MUCA}}(E) &= \exp[-\beta_0 \mathcal{E}_{\mathrm{MUCA}}(E)] \\ &= \begin{cases} \exp(-\beta_1 E) , & \text{for } E<E_1, \\ \dfrac{1}{n(E)}, & \text{for } E_1 \leq E \leq E_M, \\ \exp(-\beta_M E), & \text{for } E>E_M. \end{cases} \end{aligned} \tag{64}$$

The multicanonical MC and MD runs are then performed respectively with the Metropolis criterion of Eq. 55 and with the modified Newton equation in Eq. 57, in which $\mathcal{E}_{\mathrm{MUCA}}(E)$ in Eq. 63 is substituted into $E_{\mathrm{MUCA}}(E; T_0)$. We expect to obtain a flat potential energy distribution in the range of Eq. 61. Finally, the results are analyzed by the single-histogram reweighting techniques as described in Eq. 59 (and Eq. 30).

The formulations of REST and REMUCA are simple and straightforward, but the numerical improvement is great, because the weight factor determination for ST and MUCA becomes very difficult by the usual iterative processes for complex systems.

2.5. Simulated Tempering Replica-Exchange Method and Multicanonical Replica-Exchange Method

In the previous subsection we presented REST and REMUCA, which use a short REM run for the determination of the simulated tempering weight factor and the multicanonical weight factor, respectively. Here, we present two modifications of REM and refer to the new methods as the *STREM* (87) and *MUCAREM* (105, 109, 110). In STREM the production run is a REM simulation with a few replicas that perform ST simulations with different temperature ranges. Likewise, in MUCAREM, the production run is a REM simulation with a few replicas in multicanonical ensembles, i.e., different replicas perform MUCA simulations with different energy ranges.

While ST and MUCA simulations are usually based on local updates, a replica-exchange process can be considered to be a global update, and global updates enhance the conformational sampling further.

3. Multidimensional Extensions of the Three Generalized-Ensemble Algorithms

3.1. General Formulations

We now give the general formulations for the multidimensional generalized-ensemble algorithms (154–156). Let us consider a generalized potential energy function $E_{\boldsymbol{\lambda}}(x)$, which depends on L parameters $\boldsymbol{\lambda} = (\lambda^{(1)}, \ldots, \lambda^{(L)})$, of a system in state x. Although $E_{\boldsymbol{\lambda}}(x)$ can be any function of $\boldsymbol{\lambda}$, we consider the following specific generalized potential energy function for simplicity:

$$E_{\boldsymbol{\lambda}}(x) = E_0(x) + \sum_{\ell=1}^{L} \lambda^{(\ell)} V_\ell(x). \tag{65}$$

Here, there are $L + 1$ energy terms, $E_0(x)$ and $V_\ell(x)$ ($\ell = 1, \ldots, L$), and $\lambda^{(\ell)}$ are the corresponding coupling constants for $V_\ell(x)$.

After integrating out the momentum degrees of freedom, the partition function of the system at fixed temperature T and parameters $\boldsymbol{\lambda}$ is given by

$$\begin{aligned} Z(T, \boldsymbol{\lambda}) &= \int dx \exp(-\beta E_{\boldsymbol{\lambda}}(x)) \\ &= \int dE_0 dV_1 \cdots dV_L \; n(E_0, V_1, \ldots, V_L) \exp(-\beta E_{\boldsymbol{\lambda}}), \end{aligned} \tag{66}$$

where $n(E_0, V_1, \ldots, V_L)$ is the multidimensional density of states:

$$\begin{aligned} n(E_0, V_1, \ldots, V_L) = \int dx \delta(E_0(x) - E_0) \delta(V_1(x) \\ - V_1) \cdots \delta(V_L(x) - V_L). \end{aligned} \tag{67}$$

Here, the integration is replaced by a summation when x is discrete.

The expression in Eq. 65 is often used in simulations. For instance, in simulations of spin systems, $E_0(x)$ and $V_1(x)$ (here, $L = 1$ and $x = \{S_1, S_2, \cdots\}$ stand for spins) can be respectively considered as the zero-field term and the magnetization term coupled with the external field $\lambda^{(1)}$. (For Ising model, $E_0 = -J\sum_{,j>} S_i S_j$, $V_1 = -\sum_i S_i$, and $\lambda^{(1)} = h$, i.e., external magnetic field.) In umbrella sampling (30) in molecular simulations, $E_0(x)$ and $V_\ell(x)$ can be taken as the original potential energy and the (biasing) umbrella potential energy, respectively, with the coupling parameter $\lambda^{(\ell)}$ (here, $x = \{\boldsymbol{q}_1, \ldots, \boldsymbol{q}_N\}$ where $\boldsymbol{q}_k$ is the coordinate vector of the kth particle and N is the total number of particles). For the molecular simulations in the isobaric-isothermal ensemble, $E_0(x)$ and $V_1(x)$ (here, $L = 1$) correspond respectively to the potential energy U and the volume $\mathcal{V}$ coupled with the pressure $\mathcal{P}$. (Namely, we have $x = \{\boldsymbol{q}_1, \ldots, \boldsymbol{q}_N, \mathcal{V}\}$, $E_0 = U$, $V_1 = \mathcal{V}$, and $\lambda^{(1)} = \mathcal{P}$, i.e., $E_{\boldsymbol{\lambda}}$ is the enthalpy without the kinetic energy contributions). For simulations in the grand canonical ensemble with N particles, we have $x = \{\boldsymbol{q}_1, \ldots, \boldsymbol{q}_N, N\}$, and $E_0(x)$ and $V_1(x)$ (here, $L = 1$) correspond respectively to the potential energy U and the total number of particles N coupled with the chemical potential μ. (Namely, we have $E_0 = U$, $V_1 = N$, and $\lambda^{(1)} = -\mu$.)

Moreover, going beyond the well-known ensembles discussed above, we can introduce any physical quantity of interest (or its function) as the additional potential energy term V_ℓ. For instance, V_ℓ can be an overlap with a reference configuration in spin glass systems, an end-to-end distance, a radius of gyration in molecular systems, etc. In such a case, we have to carefully choose the range of $\lambda^{(\ell)}$ values so that the new energy term $\lambda^{(\ell)} V_\ell$ will have roughly the same order of magnitude as the original energy term E_0. We want to perform a simulation where a random walk not only in the E_0 space but also in the V_ℓ space is realized. As shown below, this can be done by performing a multidimensional REM, ST, or MUCA simulation.

We first describe the *multidimensional replica-exchange method* (MREM) (103). The crucial observation that led to this algorithm is: As long as we have M *non-interacting* replicas of the original system, the Hamiltonian $H(q, p)$ of the system does not have to be identical among the replicas and it can depend on a parameter with different parameter values for different replicas. The system for the multidimensional REM consists of M non-interacting replicas of the original system in the "canonical ensemble" with $M(= M_0 \times M_1 \times \cdots \times M_L)$ different parameter sets Λ_m $(m = 1, \ldots, M)$, where $\boldsymbol{\Lambda}_m \equiv (T_{m_0}, \boldsymbol{\lambda}_m) \equiv (T_{m_0}, \lambda^{(1)}_{m_1}, \ldots, \lambda^{(L)}_{m_L})$ with $m_0 = 1, \ldots, M_0, m_\ell = 1, \ldots, M_\ell$ $(\ell = 1, \ldots, L)$. Because the replicas are non-interacting, the weight factor is given by the product of Boltzmann-like factors for each replica:

$$W_{\mathrm{MREM}} \equiv \prod_{m_0=1}^{M_0} \prod_{m_1=1}^{M_1} \cdots \prod_{m_L=1}^{M_L} \exp\left(-\beta_{m_0} E_{\boldsymbol{\lambda}_m}\right). \tag{68}$$

Without loss of generality we can order the parameters so that $T_1 < T_2 < \cdots < T_{M_0}$ and $\lambda_1^{(\ell)} < \lambda_2^{(\ell)} < \cdots < \lambda_{M_\ell}^{(\ell)}$ (for each $\ell = 1, \ldots, L$). The multidimensional REM is realized by alternately performing the following two steps:

1. For each replica, a "canonical" MC or MD simulation at the fixed parameter set is carried out simultaneously and independently for a certain steps.
2. We exchange a pair of replicas i and j which are at the parameter sets $\boldsymbol{\Lambda}_m$ and $\boldsymbol{\Lambda}_{m+1}$, respectively. The transition probability for this replica-exchange process is given by

$$w(\boldsymbol{\Lambda}_m \leftrightarrow \boldsymbol{\Lambda}_{m+1}) = \min(1, \exp(-\Delta)), \tag{69}$$

where we have

$$\Delta = \left(\beta_{m_0} - \beta_{m_0+1}\right)\left(E_{\boldsymbol{\lambda}_m}\left(q^{[j]}\right) - E_{\boldsymbol{\lambda}_m}\left(q^{[i]}\right)\right), \tag{70}$$

for T-exchange, and

$$\Delta = \beta_{m_0}\left[\left(E_{\boldsymbol{\lambda}_{m_\ell}}(q^{[j]}) - E_{\boldsymbol{\lambda}_{m_\ell}}(q^{[i]})\right) - \left(E_{\boldsymbol{\lambda}_{m_\ell+1}}(q^{[j]}) - E_{\boldsymbol{\lambda}_{m_\ell+1}}(q^{[i]})\right)\right], \tag{71}$$

for $\lambda^{(\ell)}$-exchange (for one of $\ell = 1, \ldots, L$). Here, $q^{[i]}$ and $q^{[j]}$ stand for configuration variables for replicas i and j, respectively, before the replica exchange.

We now consider the *multidimensional simulated tempering* (MST) which realizes a random walk both in temperature T and in parameters $\boldsymbol{\lambda}$ (154–156). The entire parameter set $\boldsymbol{\Lambda} = (T, \boldsymbol{\lambda}) \equiv (T, \lambda^{(1)}, \ldots, \lambda^{(L)})$ becomes dynamical variables, and both the configuration and the parameter set are updated during the simulation with a weight factor:

$$W_{\mathrm{MST}}(\boldsymbol{\Lambda}) \equiv \exp(-\beta E_{\boldsymbol{\lambda}} + f(\boldsymbol{\Lambda})), \tag{72}$$

where the function $f(\boldsymbol{\Lambda}) = f(T, \boldsymbol{\lambda})$ is chosen so that the probability distribution of $\boldsymbol{\Lambda}$ is flat:

$$P_{\mathrm{MST}}(\boldsymbol{\Lambda}) \propto \int dE_0 dV_1 \cdots dV_L \; n(E_0, V_1, \ldots, V_L)$$
$$\exp(-\beta E_{\boldsymbol{\lambda}} + f(\boldsymbol{\Lambda})) \equiv \text{constant}. \tag{73}$$

This means that $f(\Lambda)$ is the dimensionless ("Helmholtz") free energy:

$$\exp(-f(\boldsymbol{\Lambda})) = \int dE_0 dV_1 \cdots dV_L \; n(E_0, V_1, \ldots, V_L) \; \exp(-\beta E_{\boldsymbol{\lambda}}). \tag{74}$$

In the numerical work we discretize the parameter set $\mathbf{\Lambda}$ in M $(= M_0 \times M_1 \times \cdots \times M_L)$ different values: $\mathbf{\Lambda}_m \equiv (T_{m_0}, \boldsymbol{\lambda}_m) \equiv (T_{m_0}, \lambda_{m_1}^{(1)}, \ldots, \lambda_{m_L}^{(L)})$, where $m_0 = 1, \ldots, M_0, m_\ell = 1, \ldots, M_\ell$ $(\ell = 1, \ldots, L)$. Without loss of generality we can order the parameters so that $T_1 < T_2 < \cdots < T_{M_0}$ and $\lambda_1^{(\ell)} < \lambda_2^{(\ell)} < \cdots < \lambda_{M_\ell}^{(\ell)}$ (for each $\ell = 1, \ldots, L$). The free energy $f(\mathbf{\Lambda}_m)$ is now written as $f_{m_0, m_1, \ldots, m_L} = f(T_{m_0}, \lambda_{m_1}^{(1)}, \ldots, \lambda_{m_L}^{(L)})$.

Once the initial configuration and the initial parameter set are chosen, the multidimensional ST is realized by alternately performing the following two steps:

1. A "canonical" MC or MD simulation at the fixed parameter set $\mathbf{\Lambda}_m = (T_{m_0}, \boldsymbol{\lambda}_m) = (T_{m_0}, \lambda_{m_1}^{(1)}, \ldots, \lambda_{m_L}^{(L)})$ is carried out for a certain steps with the weight factor $\exp(-\beta_{m_0} E_{\boldsymbol{\lambda}_m})$ (for fixed $\mathbf{\Lambda}_m$, $f(\mathbf{\Lambda}_m)$ in Eq. 72 is a constant and does not contribute).
2. We update the parameter set $\mathbf{\Lambda}_m$ to a new parameter set $\mathbf{\Lambda}_{m \pm 1}$ in which one of the parameters in $\mathbf{\Lambda}_m$ is changed to a neighboring value with the configuration and the other parameters fixed. The transition probability of this parameter updating process is given by the following Metropolis criterion:

$$w(\mathbf{\Lambda}_m \to \mathbf{\Lambda}_{m\pm1}) = \min\left(1, \frac{W_{\mathrm{MST}}(\mathbf{\Lambda}_{m\pm1})}{W_{\mathrm{MST}}(\mathbf{\Lambda}_m)}\right) = \min(1, \exp(-\Delta)). \tag{75}$$

Here, there are two possibilities for $\mathbf{\Lambda}_{m \pm 1}$, namely, T-update and $\lambda^{(\ell)}$-update. For T-update, we have $\mathbf{\Lambda}_{m\pm1} = (T_{m_0\pm1}, \boldsymbol{\lambda}_m)$ with

$$\Delta = (\beta_{m_0\pm1} - \beta_{m_0}) E_{\boldsymbol{\lambda}_m} - \left(f_{m_0\pm1, m_1, \ldots, m_L} - f_{m_0, m_1, \ldots, m_L}\right). \tag{76}$$

For $\boldsymbol{\lambda}^{(\ell)}$-update (for one of $\ell = 1, \ldots, L$), we have $\mathbf{\Lambda}_{m\pm1} = (T_{m_0}, \boldsymbol{\lambda}_{m_\ell\pm1})$ with

$$\Delta = \beta_{m_0}(E_{\boldsymbol{\lambda}_{m_\ell\pm1}} - E_{\boldsymbol{\lambda}_{m_\ell}}) - \left(f_{m_0, \ldots, m_\ell\pm1, \cdots} - f_{m_0, \ldots, m_\ell, \cdots}\right), \tag{77}$$

where $\boldsymbol{\lambda}_{m_\ell\pm1} = (\ldots, \lambda_{m_{\ell-1}}^{(\ell-1)}, \lambda_{m_\ell\pm1}^{(\ell)}, \lambda_{m_{\ell+1}}^{(\ell+1)}, \cdots)$ and $\boldsymbol{\lambda}_{\mathrm{m}_\ell} = (\ldots, \lambda_{\mathrm{m}_{\ell-1}}^{(\ell-1)}, \lambda_{m_\ell}^{(\ell)}, \lambda_{m_{\ell+1}}^{(\ell+1)}, \cdots)$.

We now describe the *multidimensional multicanonical algorithm* (MMUCA) which realizes a random walk in the $(L + 1)$-dimensional space of $E_0(x)$ and $V_\ell(x)$ $(\ell = 1, \ldots, L)$.

In the multidimensional MUCA ensemble, each state is weighted by the MUCA weight factor $W_{\mathrm{MMUCA}}(E_0, V_1, \ldots, V_L)$ so that a uniform energy distribution of E_0, V_1, $\cdots$, and V_L may be obtained:

$$P_{\mathrm{MMUCA}}(E_0, V_1, \ldots, V_L) \propto n(E_0, V_1, \ldots, V_L) W_{\mathrm{MMUCA}}$$
$$(E_0, V_1, \ldots, V_L) \equiv \text{constant}, \tag{78}$$

where $n(E_0, V_1, \ldots, V_L)$ is the multidimensional density of states. From this equation, we obtain

$$W_{\mathrm{MMUCA}}(E_0, V_1, \ldots, V_L) \equiv \exp(-\beta_a E_{\mathrm{MMUCA}}(E_0, V_1, \ldots, V_L)) \propto \frac{1}{n(E_0, V_1, \ldots, V_L)}, \tag{79}$$

where we have introduced an arbitrary reference temperature, $T_a = 1/k_{\mathrm{B}}\beta_a$, and wrote the weight factor in the Boltzmann-like form. Here, the "multicanonical potential energy" is defined by

$$E_{\mathrm{MMUCA}}(E_0, V_1, \ldots, V_L; T_a) \equiv k_{\mathrm{B}} T_a \ln n(E_0, V_1, \ldots, V_L). \tag{80}$$

The multidimensional MUCA MC simulation can be performed with the following Metropolis transition probability from state x with energy $E_{\boldsymbol{\lambda}} = E_0 + \sum_{\ell=1}^{L} \lambda^{(\ell)} V_\ell$ to state x' with energy $E_{\boldsymbol{\lambda}}{}' = E_0{}' + \sum_{\ell=1}^{L} \lambda^{(\ell)} V_\ell{}'$:

$$w(x \to x') = \min\left(1, \frac{W_{\mathrm{MMUCA}}(E_0{}', V_1{}', \ldots, V_L{}')}{W_{\mathrm{MMUCA}}(E_0, V_1, \ldots, V_L)}\right) = \min\left(1, \frac{n(E_0, V_1, \ldots, V_L)}{n(E_0{}', V_1{}', \ldots, V_L{}')}\right). \tag{81}$$

An MD algorithm in the multidimensional MUCA ensemble also naturally follows from Eq. 79, in which a regular constant temperature MD simulation (with $T = T_a$) is performed by replacing the total potential energy $E_{\boldsymbol{\lambda}}$ by the multicanonical potential energy E_{MMUCA} in Eq. 12:

$$\dot{\boldsymbol{p}}_k = -\frac{\partial E_{\mathrm{MMUCA}}(E_0, V_1, \ldots, V_L; T_a)}{\partial \boldsymbol{q}_k} - \frac{\dot{s}}{s}\boldsymbol{p}_k. \tag{82}$$

We remark that the random walk in E_0 and in V_ℓ for the MUCA simulation corresponds to that in β and in $\beta\lambda^{(\ell)}$ for the ST simulation:

$$\begin{cases} E_0 \longleftrightarrow \beta, \\ V_\ell \longleftrightarrow \beta\lambda^{(\ell)}, \quad (\ell = 1, \ldots, L). \end{cases} \tag{83}$$

They are in conjugate relation.

3.2. Weight Factor Determinations for Multidimensional ST and MUCA

Among the three multidimensional generalized-ensemble algorithms described above, only MREM can be performed without much preparation because the weight factor for MREM is just a product of regular Boltzmann-like factors. On the other hand, we do not know the MST and MMUCA weight factors a priori and need to estimate them. As a simple method for these weight factor determinations, we can generalize the REST and REMUCA presented in the previous subsections to multidimensions.

Suppose we have made a single run of a short MREM simulation with $M(= M_0 \times M_1 \times \cdots \times M_L)$ replicas that correspond to M

different parameter sets $\boldsymbol{\Lambda}_m$ ($m = 1, \ldots, M$). Let $N_{m_0,m_1,\ldots,m_L}(E_0, V_1, \ldots, V_L)$ and $n_{m_0,m_1,\ldots,m_L}$ be respectively the $(L+1)$-dimensional potential-energy histogram and the total number of samples obtained for the mth parameter set $\boldsymbol{\Lambda}_m = (T_{m_0}, \lambda_{m_1}^{(1)}, \ldots, \lambda_{m_L}^{(L)})$. The generalized WHAM equations are then given by

$$n(E_0, V_1, \ldots, V_L) = \frac{\sum_{m_0,m_1,\ldots,m_L} N_{m_0,m_1,\ldots,m_L}(E_0, V_1, \ldots, V_L)}{\sum_{m_0,m_1,\ldots,m_L} n_{m_0,m_1,\ldots,m_L} \exp\left(f_{m_0,m_1,\ldots,m_L} - \beta_{m_0} E_{\boldsymbol{\lambda}_m}\right)}, \tag{84}$$

and

$$\exp(-f_{m_0,m_1,\ldots,m_L}) = \sum_{E_0,V_1,\ldots,V_L} n(E_0, V_1, \ldots, V_L) \exp\left(-\beta_{m_0} E_{\boldsymbol{\lambda}_m}\right). \tag{85}$$

The density of states $n(E_0, V_1, \ldots, V_L)$ (which is inversely proportional to the MMUCA weight factor) and the dimensionless free energy $f_{m_0,m_1,\ldots,m_L}$ (which is the MST parameter) are obtained by solving Eqs. 84 and 85 self-consistently by iteration.

3.3. Expectation Values of Physical Quantities

We now present the equations to calculate ensemble averages of physical quantities with any temperature T and any parameter λ values.

After a long production run of MREM and MST simulations, the canonical expectation value of a physical quantity A with the parameter values $\boldsymbol{\Lambda}_m$ ($m = 1, \ldots, M$), where $\boldsymbol{\Lambda}_m \equiv (T_{m_0}, \boldsymbol{\lambda}_m) \equiv (T_{m_0}, \boldsymbol{\lambda}_{m_1}^{(1)}, \ldots, \boldsymbol{\lambda}_{m_L}^{(L)})$ with $m_0 = 1, \ldots, M_0, m_\ell = 1, \ldots, M_\ell$ ($\ell = 1, \ldots, L$), and $M (= M_0 \times M_1 \times \cdots \times M_L)$, can be calculated by the usual arithmetic mean:

$$<A>_{T_{m_0},\boldsymbol{\lambda}_m} = \frac{1}{n_m} \sum_{k=1}^{n_m} A(x_m(k)), \tag{86}$$

where $x_m(k)$ ($k = 1, \ldots, n_m$) are the configurations obtained with the parameter values $\boldsymbol{\Lambda}_m$ ($m = 1, \ldots, M$), and n_m is the total number of measurements made with these parameter values. The expectation values of A at any intermediate $T (= 1/k_B\beta)$ and any $\boldsymbol{\lambda}$ can also be obtained from

$$<A>_{T,\boldsymbol{\lambda}} = \frac{\sum_{E_0,V_1,\ldots,V_L} A(E_0, V_1, \ldots, V_L) n(E_0, V_1, \ldots, V_L) \exp(-\beta E_{\boldsymbol{\lambda}})}{\sum_{E_0,V_1,\ldots,V_L} n(E_0, V_1, \ldots, V_L) \exp(-\beta E_{\boldsymbol{\lambda}})}, \tag{87}$$

where the density of states $n(E_0, V_1, \ldots, V_L)$ is obtained from the multiple-histogram reweighting techniques. Namely, from the MREM or MST simulation, we first obtain the histogram

$N_{m_0,m_1,\ldots,m_L}(E_0, V_1, \ldots, V_L)$ and the total number of samples $n_{m_0,m_1,\ldots,m_L}$ in Eq. 84. The density of states $n(E_0, V_1, \ldots, V_L)$ and the dimensionless free energy $f_{m_0,m_1,\ldots,m_L}$ are then obtained by solving Eqs. 84 and 85 self-consistently by iteration. Substituting the obtained density of states $n(E_0, V_1, \ldots, V_L)$ into Eq. 87, one can calculate the ensemble average of the physical quantity A at any T and any $\boldsymbol{\lambda}$.

Moreover, the ensemble average of the physical quantity A (including those that cannot be expressed as functions of E_0 and V_ℓ ($\ell = 1, \ldots, L$) can be obtained from the "trajectory" of configurations of the production run (155). Namely, we first obtain $f_{m_0,m_1,\ldots,m_L}$ for each $(m_0 = 1, \ldots, M_0, m_1 = 1, \ldots, M_1, \ldots, m_L = 1, \ldots, M_L)$ by solving Eqs. 84 and 85 self-consistently, and then we have

$$<A>_{T,\boldsymbol{\lambda}} = \frac{\sum_{m_0=1}^{M_0} \cdots \sum_{m_L=1}^{M_L} \sum_{x_m} A(x_m) \frac{\exp(-\beta E_{\boldsymbol{\lambda}}(x_m))}{\sum_{n_0=1}^{M_0} \cdots \sum_{n_L=1}^{M_L} n_{n_0,\ldots,n_L} \exp\left(f_{n_0,\ldots,n_L} - \beta_{n_0} E_{\boldsymbol{\lambda}_n}(x_m)\right)}}{\sum_{m_0=1}^{M_0} \cdots \sum_{m_L=1}^{M_L} \sum_{x_m} \frac{\exp(-\beta E_{\boldsymbol{\lambda}}(x_m))}{\sum_{n_0=1}^{M_0} \cdots \sum_{n_L=1}^{M_L} n_{n_0,\ldots,n_L} \exp\left(f_{n_0,\ldots,n_L} - \beta_{n_0} E_{\boldsymbol{\lambda}_n}(x_m)\right)}}, \tag{88}$$

where x_m are the configurations obtained at $\boldsymbol{\Lambda}_m = (T_{m_0}, \boldsymbol{\lambda}_m) = (T_{m_0}, \lambda_{m_1}^{(1)}, \ldots, \lambda_{m_L}^{(L)})$. Here, the trajectories x_m are stored for each $\boldsymbol{\Lambda}_m$ separately.

For the MMUCA simulation with the weight factor $W_{\mathrm{MMUCA}}(E_0, \ldots, V_L)$, the expectation values of A at any $T(= 1/k_{\mathrm{B}}\beta)$ and any $\boldsymbol{\lambda}$ can also be obtained from Eq. 87 by the single-histogram reweighting techniques as follows. Let $N_{\mathrm{MMUCA}}(E_0, V_1, \ldots, V_L)$ be the histogram of the distribution of $E_0, V_1, \ldots, V_L$, $P_{\mathrm{MMUCA}}(E_0, V_1, \ldots, V_L)$, obtained by the production run. The best estimate of the density of states $n(E_0, V_1, \ldots, V_L)$ is then given by

$$n(E_0, V_1, \ldots, V_L) = \frac{N_{\mathrm{MMUCA}}(E_0, V_1, \ldots, V_L)}{W_{\mathrm{MMUCA}}(E_0, \ldots, V_L)}. \tag{89}$$

Moreover, the ensemble average of the physical quantity A (including those that cannot be expressed as a function of E_0 and V_ℓ ($\ell = 1, \ldots, L$)) can be obtained as long as one stores the "trajectory" of configurations x_k from the production run. We have

$$<A>_{T,\boldsymbol{\lambda}} = \frac{\sum_{k=1}^{n_s} A(x_k) W_{\mathrm{MMUCA}}^{-1}(E_0(x_k), \ldots, V_L(x_k)) \exp(-\beta E_{\boldsymbol{\lambda}}(x_k))}{\sum_{k=1}^{n_s} W_{\mathrm{MMUCA}}^{-1}(E_0(x_k), \ldots, V_L(x_k)) \exp(-\beta E_{\boldsymbol{\lambda}}(x_k))}. \tag{90}$$

Here, x_k is the configuration at the kth MC (or MD) step and n_s is the total number of configurations stored.

3.4. Multidimensional Generalized-Ensemble Algorithms for the Isobaric–Isothermal Ensemble

As examples of the multidimensional formulations in the previous subsections, we present the generalized-ensemble algorithms for the isobaric-isothermal ensemble (or, the NPT ensemble) (157). Let us consider a physical system that consists of N atoms and that is in a box of a finite volume $\mathcal{V}$. The states of the system are specified by coordinates $q \equiv \{\boldsymbol{q}_1, \boldsymbol{q}_2, \ldots, \boldsymbol{q}_N\}$ and momenta $p \equiv \{\boldsymbol{p}_1, \boldsymbol{p}_2, \ldots, \boldsymbol{p}_N\}$ of the atoms and volume $\mathcal{V}$ of the box. The potential energy $E(q, \mathcal{V})$ for the system is a function of q and $\mathcal{V}$.

In the isobaric-isothermal ensemble (159, 160, 165, 172), the probability distribution $P_{\mathrm{NPT}}(E, \mathcal{V}; T, \mathcal{P})$ for potential energy E and volume $\mathcal{V}$ at temperature T and pressure $\mathcal{P}$ is given by

$$P_{\mathrm{NPT}}(E, \mathcal{V}; T, \mathcal{P}) \propto n(E, \mathcal{V}) W_{\mathrm{NPT}}(E, \mathcal{V}; T, \mathcal{P}) = n(E, \mathcal{V}) e^{-\beta \mathcal{H}}. \tag{91}$$

Here, the density of states $n(E, \mathcal{V})$ is given as a function of both E and $\mathcal{V}$, and $\mathcal{H}$ is the "enthalpy" (without the kinetic energy contributions):

$$\mathcal{H} = E + \mathcal{P}\mathcal{V}. \tag{92}$$

This weight factor produces an isobaric-isothermal ensemble at constant temperature (T) and constant pressure ($\mathcal{P}$). Note that this is a special case of the general formulations in Eq. 7.65 with $L = 1$, $E_0 = E$, $V_1 = \mathcal{V}$, and $\lambda^{(1)} = \mathcal{P}$.

In order to perform the isobaric-isothermal MC simulation (172), we perform Metropolis sampling on the scaled coordinates $\sigma = \{\boldsymbol{\sigma}_1, \boldsymbol{\sigma}_2, \ldots, \boldsymbol{\sigma}_N\}$ where $\boldsymbol{\sigma}_k = \mathcal{V}^{-1/3} \boldsymbol{q}_k (k = 1, 2, \ldots, N)$ ($\boldsymbol{q}_k$ are the real coordinates) and the volume $\mathcal{V}$ (here, the particles are placed in a cubic box of a side of size $\mathcal{V}^{-1/3}$). The trial moves from state x with the scaled coordinate σ with volume $\mathcal{V}$ to state x' with the scaled coordinate σ' and volume $\mathcal{V}'$ are generated by uniform random numbers. The enthalpy is accordingly changed from $\mathcal{H}(E(\sigma, \mathcal{V}), \mathcal{V})$ to $\mathcal{H}'(E(\sigma', \mathcal{V}'), \mathcal{V}')$ by these trial moves. The trial moves will be accepted with the following Metropolis criterion:

$$w(x \to x') = \min(1, \exp[-\beta\{\mathcal{H}' - \mathcal{H} - N k_B T \ln(\mathcal{V}'/\mathcal{V})\}]), \tag{93}$$

where N is the total number of atoms in the system.

As for the MD method in this ensemble, we just present the Nosé-Andersen algorithm (159, 160, 165). The equations of motion in Eqs. 11–14 are now generalized as follows:

$$\dot{\boldsymbol{q}}_k = \frac{\boldsymbol{p}_k}{m_k} + \frac{\dot{\mathcal{V}}}{3\mathcal{V}} \boldsymbol{q}_k, \tag{94}$$

$$\dot{\boldsymbol{p}}_k = -\frac{\partial \mathcal{H}}{\partial \boldsymbol{q}_k} - \left(\frac{\dot{s}}{s} + \frac{\dot{\mathcal{V}}}{3\mathcal{V}}\right)\boldsymbol{p}_k \tag{95}$$

$$= \boldsymbol{f}_k - \left(\frac{\dot{s}}{s} + \frac{\dot{\mathcal{V}}}{3\mathcal{V}}\right)\boldsymbol{p}_k, \tag{96}$$

$$\dot{s} = s\ \frac{P_s}{Q}, \tag{97}$$

$$\dot{P}_s = \sum_{i=1}^{N} \frac{\boldsymbol{p}_i^2}{m_i} - 3Nk_{\mathrm{B}}T\ =\ 3Nk_{\mathrm{B}}(T(t) - T), \tag{98}$$

$$\dot{\mathcal{V}} = s\ \frac{P_{\mathcal{V}}}{\mathcal{M}}, \tag{99}$$

$$\dot{P}_{\mathcal{V}} = s\left[\frac{1}{3\mathcal{V}}\left(\sum_{i=1}^{N} \frac{\boldsymbol{p}_i^2}{m_i} - \sum_{i=1}^{N} \boldsymbol{q}_i \cdot \frac{\partial \mathcal{H}}{\partial \boldsymbol{q}_i}\right) - \frac{\partial \mathcal{H}}{\partial \mathcal{V}}\right] \tag{100}$$

$$= s(\mathcal{P}(t) - \mathcal{P}), \tag{101}$$

where $\mathcal{M}$ is the artificial mass associated with the volume, $P_{\mathcal{V}}$ is the conjugate momentum for the volume, and the "instantaneous pressure" $\mathcal{P}(t)$ is defined by

$$\mathcal{P}(t) = \frac{1}{3\mathcal{V}}\left(\sum_{i=1}^{N} \frac{\boldsymbol{p}_i(t)^2}{m_i} + \sum_{i=1}^{N} \boldsymbol{q}_i(t) \cdot \boldsymbol{f}_i(t)\right) - \frac{\partial E}{\partial \mathcal{V}}(t). \tag{102}$$

In REM simulations for the NPT ensemble, we prepare a system that consists of $M_T \times M_{\mathcal{P}}$ noninteracting replicas of the original system, where M_T and $M_{\mathcal{P}}$ are the number of temperature and pressure values used in the simulation, respectively. The replicas are specified by labels $i (i = 1, 2, \ldots, M_T \times M_{\mathcal{P}})$, temperature by m_0 ($m_0 = 1, 2, \ldots, M_T$), and pressure by $m_1 (m_1 = 1, 2, \ldots, M_{\mathcal{P}})$.

To perform REM simulations, we carry out the following two steps alternately: (1) perform a usual constant NPT MC or MD simulation in each replica at assigned temperature and pressure and (2) try to exchange the replicas. If the temperature (specified by m_0 and n_0) or pressure (specified by m_1 and n_1) between the replicas is exchanged in Step 2, the transition probability from $X \equiv \{\ldots, (\sigma^{[i]}, \mathcal{V}^{[i]}; T_{m_0}, \mathcal{P}_{m_1}), \ldots, (\sigma^{[j]}, \mathcal{V}^{[j]}; T_{n_0}, \mathcal{P}_{n_1}), \cdots\}$ to $X' \equiv \{\ldots, (\sigma^{[i]}, \mathcal{V}^{[i]}; T_{n_0}, \mathcal{P}_{n_1}), \ldots, (\sigma^{[j]}, \mathcal{V}^{[j]}; T_{m_0}, \mathcal{P}_{m_1}), \cdots\}$ at the trial is given by (11, 120)

$$w_{\mathrm{REM}}(X \to X') = \min[1, \exp(-\Delta_{\mathrm{REM}})], \tag{103}$$

where

$$\Delta_{\mathrm{REM}} = (\beta_{m_0} - \beta_{n_0})\left[E\left(\sigma^{[j]}, \mathcal{V}^{[j]}\right) - E\left(\sigma^{[i]}, \mathcal{V}^{[i]}\right)\right] + (\beta_{m_0}\mathcal{P}_{m_1} - \beta_{n_0}\mathcal{P}_{n_1})\left(\mathcal{V}^{[j]} - \mathcal{V}^{[i]}\right). \tag{104}$$

In ST simulations for the NPT ensemble, we introduce a function $f(T,\mathcal{P})$ and use a weight factor $W_{\mathrm{ST}}(E,\mathcal{V};T,\mathcal{P}) \equiv \exp[-\beta(E+\mathcal{P}\mathcal{V})+f(T,\mathcal{P})]$ so that the distribution function $P_{\mathrm{ST}}(T,\mathcal{P})$ of T and $\mathcal{P}$ may be uniform:

$$P_{\mathrm{ST}}(T,\mathcal{P}) \propto \int_0^\infty d\mathcal{V} \int_{\mathcal{V}} dq\ W_{\mathrm{ST}}[E(q,\mathcal{V}),\mathcal{V};T,\mathcal{P}] = \text{constant}. \tag{105}$$

From Eq. 105, it is found that $f(T,\mathcal{P})$ is formally given by

$$f(T,\mathcal{P}) = -\ln\left\{\int_0^\infty d\mathcal{V} \int_{\mathcal{V}} dq \exp[-\beta(E(q,\mathcal{V})+\mathcal{P}\mathcal{V})]\right\}, \tag{106}$$

and this function is the dimensionless Gibbs free energy except for a constant.

To perform ST simulations, we again discretize temperature and pressure into $M_0 \times M_1$ set of values $(T_{m_0},\mathcal{P}_{m_1})(m_0 = 1,\ldots,M_0,\ m_1 = 1,\ldots,M_1)$. We carry out the following two steps alternately: (1) perform a usual constant NPT MC or MD simulation and (2) try to update the temperature or pressure. In Step 2 the transition probability from the state $X \equiv \{\sigma,\mathcal{V};T_{m_0},\mathcal{P}_{m_1}\}$ to the state $X' \equiv \{\sigma,\mathcal{V};T_{n_0},\mathcal{P}_{n_1}\}$ is given by

$$w_{\mathrm{ST}}(X \to X') = \min[1,\exp(-\Delta_{\mathrm{ST}})], \tag{107}$$

where

$$\Delta_{\mathrm{ST}} = (\beta_{n_0}-\beta_{m_0})E(\sigma,\mathcal{V}) + (\beta_{n_0}\mathcal{P}_{n_1}-\beta_{m_0}\mathcal{P}_{m_1})\mathcal{V} - \left(f_{n_0,n_1}-f_{m_0,m_1}\right). \tag{108}$$

We remark that when we perform MD simulations with REM and ST, the momenta should be rescaled if the replicas are exchanged for the temperature in REM and the temperature is updated in ST as shown above in the previous subsections.

From the production run of REM or ST simulations in the NPT ensemble, we can calculate isobaric-isothermal averages of a physical quantity A at $(T_{m_0},\mathcal{P}_{m_1})(m_0 = 1,\ldots,M_0,\ m_1 = 1,\ldots,M_1)$ by the usual arithmetic mean:

$$<A>_{T_{m_0},\mathcal{P}_{m_1}} = \frac{1}{n_m}\sum_{k=1}^{n_m} A(x_m(k)), \tag{109}$$

where $x_m(k)$ $(k = 1, \ldots, n_m)$ are the configurations obtained with the parameter values $(T_{m_0},\mathcal{P}_{m_1})$ and n_m is the total number of measurements made with these parameter values. The expectation values of A at any intermediate temperature $T(=1/k_{\mathrm{B}}\beta)$ and any intermediate pressure $\mathcal{P}$ can also be obtained from

$$<A>_{T,\mathcal{P}} = \frac{\sum_{E,\mathcal{V}} A(E,\mathcal{V}) n(E,\mathcal{V}) \exp(-\beta(E+\mathcal{P}\mathcal{V}))}{\sum_{E,\mathcal{V}} n(E,\mathcal{V}) \exp(-\beta(E+\mathcal{P}\mathcal{V}))}, \tag{110}$$

where the density of states $n(E,\mathcal{V})$ is obtained from the multiple-histogram reweighting techniques. Namely, from the REM or ST simulation, we first obtain the histogram $N_{m_0,m_1}(E,\mathcal{V})$ and the total number of samples n_{m_0,m_1}. The density of states $n(E,\mathcal{V})$ and the dimensionless free energy f_{m_0,m_1} are then obtained by solving the following equations self-consistently by iteration (see Eqs. 84 and 85 above):

$$n(E,\mathcal{V}) = \frac{\sum_{m_0,m_1} N_{m_0,m_1}(E,\mathcal{V})}{\sum_{m_0,m_1} n_{m_0,m_1} \exp\left(f_{m_0,m_1} - \beta_{m_0}(E+\mathcal{P}_{m_1}\mathcal{V})\right)}, \tag{111}$$

and

$$\exp(-f_{m_0,m_1}) = \sum_{E,\mathcal{V}} n(E,\mathcal{V}) \exp\left(-\beta_{m_0}(E+\mathcal{P}_{m_1}\mathcal{V})\right). \tag{112}$$

Substituting the obtained density of states $n(E,\mathcal{V})$ into Eq. 110, one can calculate the ensemble average of the physical quantity A at any T and any $\mathcal{P}$.

We now introduce the MUCA into the isobaric-isothermal ensemble and refer to this generalized-ensemble algorithm as the MUBATH (72–75). The molecular simulations in this generalized ensemble perform random walks both in the potential energy space and in the volume space.

In the MUBATH ensemble, each state is sampled by the MUBATH weight factor $W_{\mathrm{mbt}}(E,\mathcal{V}) \equiv \exp\{-\beta_a \mathcal{H}_{\mathrm{mbt}}(E,\mathcal{V})\}$ ($\mathcal{H}_{\mathrm{mbt}}$ is referred to as the multibaric-multithermal enthalpy) so that a uniform distribution in both potential energy E and volume $\mathcal{V}$ is obtained (72):

$$\begin{aligned} P_{\mathrm{mbt}}(E,\mathcal{V}) &\propto n(E,\mathcal{V}) W_{\mathrm{mbt}}(E,\mathcal{V}) \\ &= n(E,\mathcal{V}) \exp\{-\beta_a \mathcal{H}_{\mathrm{mbt}}(E,\mathcal{V})\} \equiv \text{constant}, \end{aligned} \tag{113}$$

where we have chosen an arbitrary reference temperature, $T_a = 1/k_{\mathrm{B}}\beta_a$.

The MUBATH MC simulation can be performed by replacing $\mathcal{H}$ by $\mathcal{H}_{\mathrm{mbt}}$ in Eq. 93:

$$w(x \to x') = \min(1, \exp[-\beta_a\{\mathcal{H}'_{\mathrm{mbt}} - \mathcal{H}_{\mathrm{mbt}} - Nk_{\mathrm{B}}T_a \ln(\mathcal{V}'/\mathcal{V})\}]). \tag{114}$$

In order to perform the MUBATH MD simulation, we just solve the above equations of motion (Eqs. 94–101) for the regular isobaric-isothermal ensemble (with arbitrary reference temperature $T = T_a$), where the enthalpy $\mathcal{H}$ is replaced by the multibaric-multithermal enthalpy $\mathcal{H}_{\mathrm{mbt}}$ in Eqs. 95 and 100 (74).

In order to calculate the isobaric-isothermal-ensemble averages, we employ the single-histogram reweighting techniques (17, 18). The expectation value of a physical quantity A at any T and any $\mathcal{P}$ is obtained by substituting the following density of states into Eq. 110:

$$n(E,\mathcal{V}) = \frac{N_{\mathrm{mbt}}(E,\mathcal{V})}{W_{\mathrm{mbt}}(E,\mathcal{V})}, \tag{115}$$

where $N_{\mathrm{mbt}}(E,\mathcal{V})$ is the histogram of the probability distribution $P_{\mathrm{mbt}}(E,\mathcal{V})$ of potential energy and volume that was obtained by the MUBATH production run.

4. Examples of Simulation Results

We tested the effectiveness of the generalized-ensemble algorithms by using a system of a 17-residue fragment of ribonuclease T_1 (in Refs. (110, 173)) (154–156). It is known by experiments that this peptide fragment forms α-helical conformations (173). We have performed a two-dimensional REM simulation and a two-dimensional ST simulation. In these simulations, we used the following energy function:

$$E_\lambda = E_0 + \lambda E_{SOL}, \tag{116}$$

where we set $L = 1$, $V_1 = E_{SOL}$, and $\lambda^{(1)} = \lambda$ in Eq. 65. Here, E_0 is the potential energy of the solute and E_{SOL} is the solvation free energy. The parameters in the conformational energy as well as the molecular geometry were taken from ECEPP/2 (174–176).

The solvation term E_{SOL} is given by the sum of terms that are proportional to the solvent-accessible surface area of heavy atoms of the solute (177). For the calculations of solvent-accessible surface area, we used the computer code NSOL (178).

The computer code KONF90 (7, 8) was modified in order to accommodate the generalized-ensemble algorithms. The simulations were started from randomly generated conformations. We prepared eight temperatures ($M_0 = 8$) which are distributed exponentially between $T_1 = 300$ K and $T_{M_0} = 700$ K (i.e., 300.00, 338.60, 382.17, 431.36, 486.85, 549.49, 620.20, and 700.00 K) and four equally spaced λ values ($M_1 = 4$) ranging from 0 to 1 (i.e., $\lambda_1 = 0$, $\lambda_2 = 1/3$, $\lambda_3 = 2/3$, and $\lambda_4 = 1$) in the two-dimensional REM simulation and the two-dimensional ST simulation. Simulations with $\lambda = 0$ (i.e., $E_\lambda = E_0$) and with $\lambda = 1$ (i.e., $E_\lambda = E_0 + E_{SOL}$) correspond to those in gas phase and in aqueous solution, respectively.

We first present the results of the two-dimensional REM simulation. We used 32 replicas with the eight temperature values and the four λ values given above. Before taking the data, we made the two-dimensional REM simulation of 100,000 MC sweeps with each replica for thermalization. We then performed the

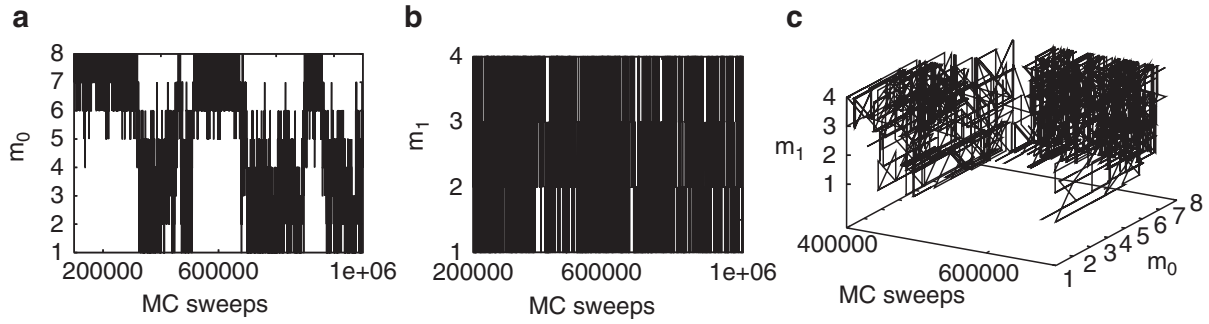

Fig. 1. Time series of the labels of T_{m_0}, m_0, (**a**) and λ_{m_1}, m_1, (**b**) as functions of MC sweeps, and that of both m_0 and m_1 for the region from 400,000 MC sweeps to 700,000 MC sweeps (**c**). The results were from one of the replicas (Replica 1). In (a) and (b), MC sweeps start at 100,000 and end at 1,100,000 because the first 100,000 sweeps have been removed from the consideration for thermalization purpose.

two-dimensional REM simulation of 1,000,000 MC sweeps for each replica to determine the weight factor for the two-dimensional ST simulation. At every 20 MC sweeps, either T-exchange or λ-exchange was tried (the choice of T or λ was made randomly). In each case, either set of pairs of replicas $((1,2),\ldots,(M-1,M))$ or $((2,3),\ldots,(M,1))$ was also chosen randomly, where M is M_0 and M_1 for T-exchange and λ-exchange, respectively.

In Fig. 1 we show the time series of labels of T_{m_0} (i.e., m_0) and λ_{m_1} (i.e., m_1) for one of the replicas. The replica realized a random walk not only in temperature space but also in λ space. The behavior of T and λ for other replicas was also similar (see Ref. (156)). From Fig. 1, one finds that the λ-random walk is more frequent than the T-random walk.

We also show the time series of temperature T, total energy E_{TOT}, conformational energy E_{C}, solvation free energy E_{SOL}, and end-to-end distance D for the same replica in Fig. 2. From Figs. 2 (a) and 2(e), we find that at lower temperatures the end-to-end distance is about 8 Å, which is the length of a fully α-helical conformation, and that at higher temperatures it fluctuates much for a range from 7 Å to 14 Å. It suggests that α-helix structures exist at low temperatures and random-coil structures occur at high temperatures. There are transitions from/to α-helix structures to/from random coils during the simulation. It indicates that the REM simulation avoided getting trapped in local-minimum-energy states and sampled a wide conformational space.

The canonical probability distributions of E_{TOT} and E_{SOL} at the 32 conditions obtained from the two-dimensional REM simulation are shown in Fig. 3. For an optimal performance of the REM simulation, there should be enough overlaps between all pairs of neighboring distributions, which will lead to sufficiently uniform and large acceptance ratios of replica exchanges. There are indeed ample overlaps between the neighboring distributions in Fig. 3.

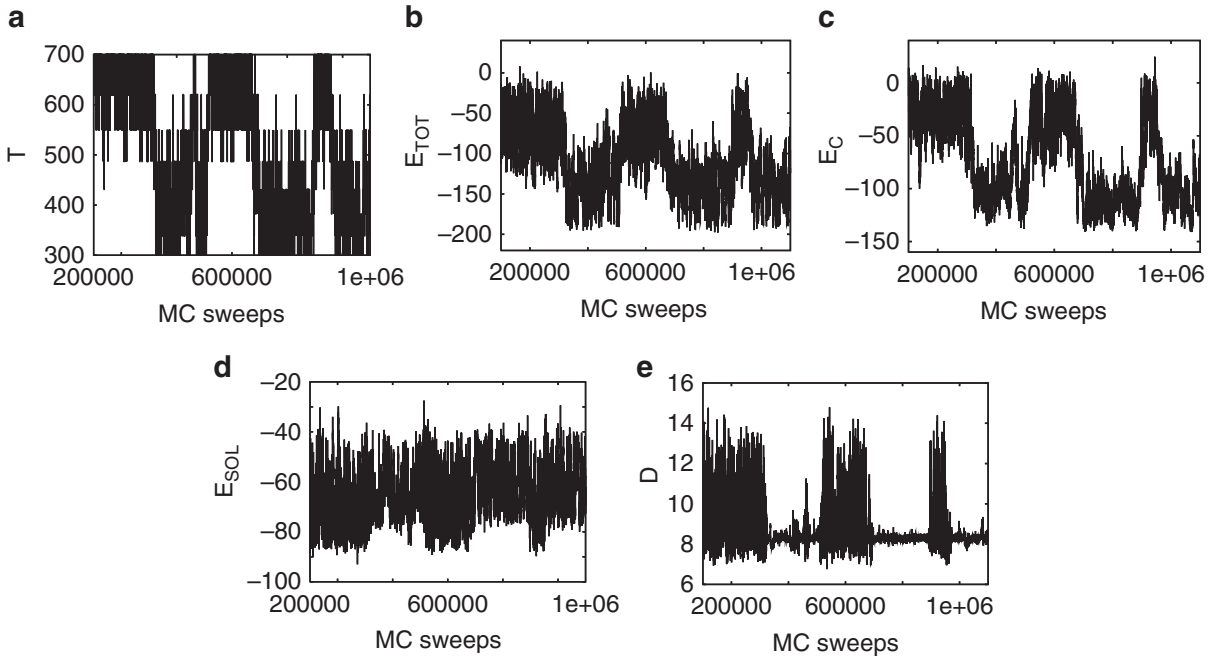

Fig. 2. Time series of the temperature T (**a**), total energy E_{TOT} (**b**), conformational energy E_C (**c**), solvation free energy E_{SOL} (**d**), and end-to-end distance D (**e**) for the same replica as in Fig. 1. The temperature is in K, the energy is in kcal/mol, and the end-to-end distance is in Å.

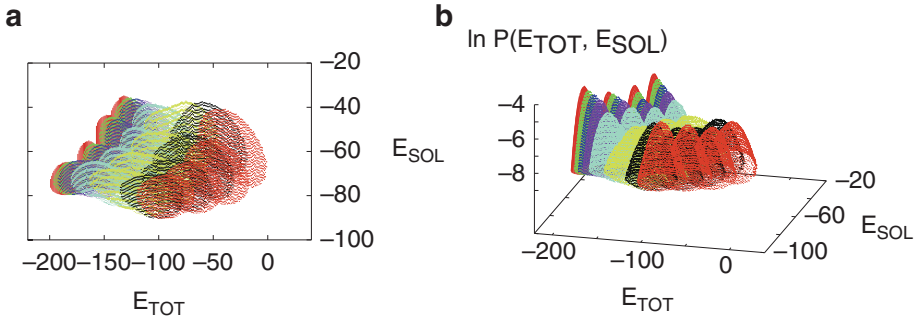

Fig. 3. Contour curves and histograms of distributions of the total energy E_{TOT} and the solvation free energy E_{SOL} ((**a**) and (**b**)) from the two-dimensional REM simulation.

We now use the results of the two-dimensional REM simulation to determine the weight factors for the two-dimensional ST simulation by the multiple-histogram reweighting techniques. Namely, by solving the generalized WHAM equations in Eqs. 84 and 85 with the obtained histograms at the 32 conditions (see Fig. 3), we obtained 32 values of the ST parameters $f_{m_0,m_1}(m_0 = 1,\ldots,8; m_1 = 1,\ldots,4)$.

After obtaining the ST weight factor, $W_{ST} = \exp(-\beta_{m_0}(E_C + \lambda_{m_1} E_{SOL}) + f_{m_0,m_1})$, we carried out the two-dimensional ST simulation of 1,000,000 MC sweeps for data collection after 100,000 MC sweeps for thermalization. At every 20 MC sweeps, either T_{m_0} or λ_{m_1} was respectively updated to $T_{m_0\pm1}$ or $\lambda_{m_1\pm1}$ (the choice of T or λ update and the choice of $\pm$ 1 were made randomly).

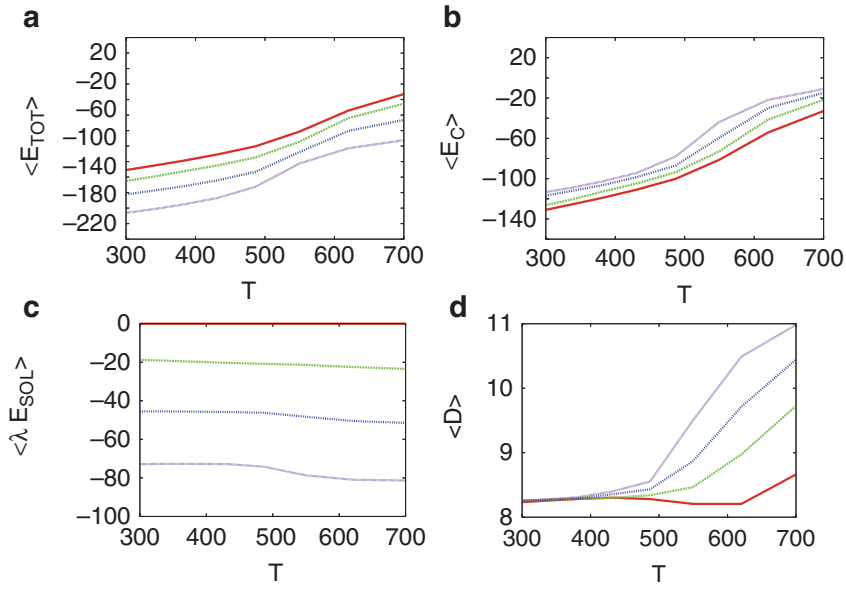

Fig. 4. The average total energy (**a**), average conformational energy (**b**), average of $\lambda \times E_{SOL}$ (**c**), and average end-to-end distance (**d**) with all the λ values as functions of temperature. The lines colored in red, green, blue, and purple are for λ_1, λ_2, λ_3, and λ_4, respectively. They are in order from above to below in (a) and (c) and from below to above in (b) and (d).

We show the average total energy, average conformational energy, average $\lambda \times E_{SOL}$, and average end-to-end distance in Fig. 4. The results are in good agreement with those of the REM simulation (data not shown).

We found that the results of the two-dimensional ST simulation are in complete agreement with those of the two-dimensional REM simulation for the average quantities. The only difference between the two simulations is the number of replicas. In the present simulation, while the REM simulation used 32 replicas, the ST simulation used only one replica. Hence, we can save much computer power with ST.

A second example of our multidimensional generalized-ensemble simulations is a pressure ST (PST) simulation in the isobaric-isothermal ensemble (157). This simulation performs a random walk in one-dimensional pressure space. The system that we simulated is ubiquitin in explicit water. This system has been studied by high-pressure NMR experiments and known to undergo high-pressure denaturations (179, 180). Ubiquitin has 76 amino acids and it was placed in a cubic box of 6,232 water molecules. Temperature was fixed to be 300 K throughout the simulations, and we prepared 100 values of pressure ranging from 1 bar to 10,000 bar. Temperature and pressure were controlled by Hoover-Langevin method (181), and particle mesh Ewald method (182, 183) was employed for electrostatic interactions. The time step was 2.0 fsec. The force field CHARMM22 (184) with CMAP

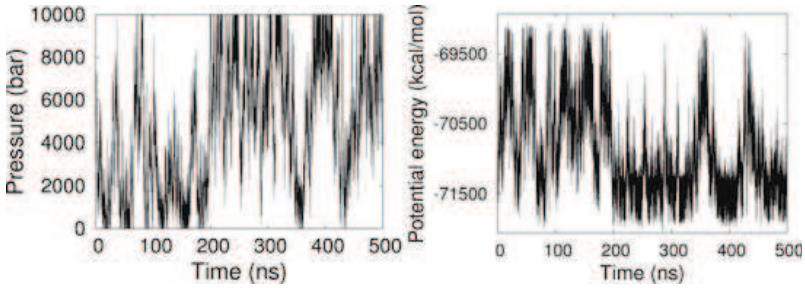

Fig. 5. Time series of pressure (*left*) and potential energy (*right*) during the PST production run.

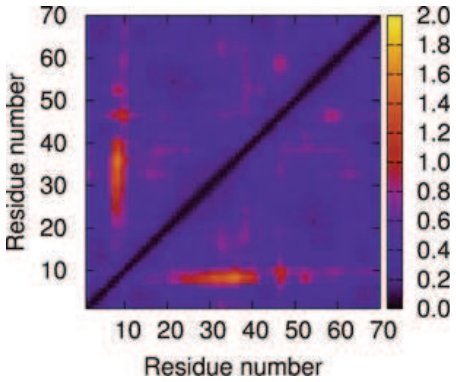

Fig. 6. Fluctuations of distance between pairs of C^{α} atoms that was calculated from the PST production run.

(185, 186) and TIP3P water model (184, 187) were used, and the program package NAMD version 2.7b3 (188) was modified to incorporate the PST algorithm.

We first performed 100 independent conventional isobaric-isothermal simulations of 4 nsec with $T = 300$ K (i.e., $M_0 = 1$) and 100 values of pressure (i.e., $M_1 = 100$). Using the obtained histogram $N_{m_0,m_1}(E, \mathcal{V})$ of potential energy and volume distribution, we obtained the ST parameters f_{m_0,m_1} by solving the WHAM equations in Eqs. 111 and 112. We then performed the PST production of 500 nsec and repeated it 10 times with different seeds for random numbers (so, the total simulation time for the production run is 5.0 μs).

In Fig. 5, we show the time series of pressure and potential energy during the PST production run.

In the figure, we see a random walk in pressure between 1 bar and 10,000 bar. A random walk in potential energy is also observed, and it is anti-correlated with that of pressure, as it should be.

We calculated the fluctuations $\sqrt{<d^2> - <d>^2}$ of the distance d between pairs of C^{α} atoms. The results are shown in Fig. 6.

We see that large fluctuations are observed between residues around 7–10 and around 20–40, which are in accord with the experimental results (179, 180).

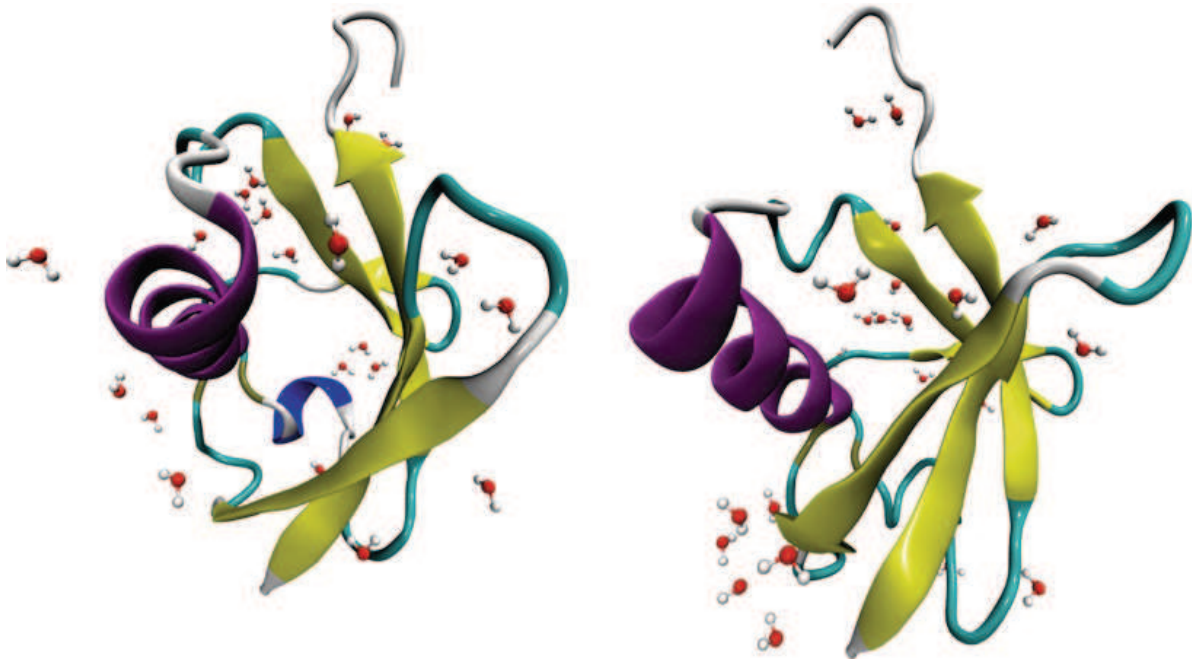

Fig. 7. Snapshots of ubiquitin during the PST production run at low pressure (*left*) and at high pressure (*right*).

The fluctuating distance corresponds to that between the turn region of the β-hairpin and the end of the α-helix as depicted in Fig. 7. While at low pressure this distance is small, at high pressure it is larger and water comes into the created open region.

5. Conclusions

In this article we first introduced three well-known generalized-ensemble algorithms, namely, REM, ST, and MUCA, which can greatly enhance conformational sampling of biomolecular systems. We then presented various extensions of these algorithms. Examples are the general formulations of the multidimensional REM, ST, and MUCA. We generalized the original potential energy function E_0 by adding any physical quantities V_ℓ of interest as a new energy term with a coupling constant $\lambda^{(\ell)}(\ell = 1, \ldots, L)$. The simulations in multidimensional REM and multidimensional ST algorithms realize a random walk in temperature and $\lambda^{(\ell)}(\ell = 1, \ldots, L)$ spaces. On the other hand, the simulation in multidimensional MUCA algorithms realizes a random walk in $E_0, V_1, \ldots, V_L$ spaces.

While the multidimensional REM simulation can be easily performed because no weight factor determination is necessary, the required number of replicas can be quite large and computationally demanding. We thus prefer to use the multidimensional ST or MUCA, where only a single replica is simulated, instead of REM. However, it is very difficult to obtain optimal weight factors

for the multidimensional ST and MUCA. Here, we have proposed a powerful method to determine these weight factors. Namely, we first perform a short multidimensional REM simulation and use the multiple-histogram reweighting techniques to determine the weight factors for multidimensional ST and MUCA simulations.

The multidimensional generalized-ensemble algorithms that were presented in the present article will be very useful for Monte Carlo and molecular dynamics simulations of complex systems such as spin glass, polymer, and biomolecular systems.

Acknowledgments

Some of the results were obtained by the computations on the supercomputersat the Institute for Molecular Science, Okazaki, and the Institute for Solid State Physics, University of Tokyo, Japan. This work was supported, in part, by Grants-in-Aid for Scientific Research on Innovative Areas ("Fluctuations and Biological Functions") and for the Next-Generation Super Computing Project, Nanoscience Program, and Computational Materials Science Initiative from the Ministry of Education, Culture, Sports, Science and Technology (MEXT), Japan.

References

1. Kirkpatrick S, Gelatt CD Jr, Vecchi MP (1983) Optimization by simulated annealing. Science 220:671–680
2. Nilges M, Clore GM, Gronenborn AM (1988) Determination of three-dimensional structures of proteins from interproton distance data by hybrid distance geometry-dynamical simulated annealing calculations. FEBS Lett 229:317–324
3. Brünger AT (1988) Crystallographic refinement by simulated annealing. Application to a 2.8 Å resolution structure of aspartate aminotransferase. J Mol Biol 203:803–816
4. Wilson SR, Cui W, Moskowitz JW, Schmidt KE (1988) Conformational analysis of flexible molecules—location of the global minimum energy conformation by the simulated annealing method. Tetrahedron Lett 29:4373–4376
5. Kawai H, Kikuchi T, Okamoto Y (1989) A prediction of tertiary structures of peptide by the Monte Carlo simulated annealing method. Protein Eng 3:85–94
6. Wilson C, Doniach S (1989) A computer model to dynamically simulate protein folding: studies with crambin. Proteins 6:193–209
7. Kawai H, Okamoto Y, Fukugita M, Nakazawa T, Kikuchi T (1991) Prediction of α-helix folding of isolated C-peptide of ribonuclease A by Monte Calro simulated annealing. Chem Lett 1991:213–216
8. Okamoto Y, Fukugita M, Nakazawa T, Kawai H (1991) α-helix folding by Monte Carlo simulated annealing in isolated C-peptide of ribonuclease A. Protein Eng 4:639–647
9. Hansmann UHE, Okamoto Y (1999) Generalized-ensemble approach for protein folding simulations. In: Stauffer D (ed) Annual Reviews of Computational Physics VI. World Scientific, Singapore, pp 129–157
10. Mitsutake A, Sugita Y, Okamoto Y (2001) Generalized-ensemble algorithms for molecular simulations of biopolymers. Biopolymers 60:96–123
11. Sugita Y, Okamoto Y (2002) Free-energy calculations in protein folding by generalized-ensemble algorithms. In: Schlick T, Gan HH (eds) Lecture notes in computational science and engineering. Springer, Berlin, pp 304–332. e-print: cond-mat/0102296

12. Okamoto Y (2004) Generalized-ensemble algorithms: enhanced sampling techniques for Monte Carlo and molecular dynamics simulations. J Mol Graphics Mod 22:425–439. e-print: cond-mat/0308360
13. Kokubo H, Okamoto Y (2006) Replica-exchange methods and predictions of helix configurations of membrane proteins. Mol Sim 32:791–801
14. Itoh SG, Okumura H, Okamoto Y (2007) Generalized-ensemble algorithms for molecular dynamics simulations. Mol Sim 33:47–56
15. Sugita Y, Mitsutake A, Okamoto Y (2008) Generalized-ensemble algorithms for protein folding simulations. In: Janke W (ed) Lecture notes in physics. Rugged free energy landscapes: common computational approaches in spin glasses, structural glasses and biological macromolecules. Springer, Berlin, pp 369–407. e-print: arXiv:0707.3382v1 [cond-mat.stat-mech]
16. Okamoto Y (2009) Generalized-ensemble algorithms for studying protein folding. In: Kuwajima K, Goto Y, Hirata F, Kataoka M, Terazima M (eds) Water and Biomolecules. Springer, Berlin, pp 61–95
17. Ferrenberg AM, Swendsen RH (1988) New Monte Carlo technique for studying phase transitions. Phys Rev Lett 61:2635–2638
18. Ferrenberg AM, Swendsen RH (1989) New Monte Carlo technique for studying phase transitions errata. Phys Rev Lett 63:1658
19. Ferrenberg AM, Swendsen RH (1989) Optimized Monte Carlo data analysis. Phys Rev Lett 63:1195–1198
20. Kumar S, Bouzida D, Swendsen RH, Kollman PA, Rosenberg JM (1992) The weighted histogram analysis method for free-energy calculations on biomolecules. 1. The method. J Comput Chem 13:1011–1021
21. Berg BA, Neuhaus T (1991) Multicanonical algorithms for 1st order phase transitions. Phys Lett B267:249–253
22. Berg BA, Neuhaus T (1992) Multicanonical ensemble: a new approach to simulate first-order phase transitions. Phys Rev Lett 68:9–12
23. Berg BA (2004) Introduction to Monte Carlo simulations and their statistical analysis. World Scientific, Singapore
24. Janke W (1998) Multicanonical Monte Carlo simulations. Phys A 254:164–178
25. Lee J (1993) New Monte Carlo algorithm: entropic sampling. Phys Rev Lett 71:211–214
26. Lee J (1993) New Monte Carlo algorithm: entropic sampling errata. Phys Rev Lett 71:2353
27. Hao WH, Scheraga HA (1994) Monte Carlo simulation of a first-order transition for protein folding. J Phys Chem 98:4940–4948
28. Mezei M (1987) Adaptive umbrella sampling—self-consistent determination of the non-Boltzmann bias. J Comput Phys 68:237–248
29. Bartels C, Karplus M (1998) Probability distributions for complex systems: adaptive umbrella sampling of the potential energy. J Phys Chem B 102:865–880
30. Torrie GM, Valleau JP (1977) Nonphysical sampling distributions in Monte Carlo free-energy estimation: umbrella sampling. J Comput Phys 23:187–199
31. Wang F, Landau DP (2001) Efficient, multiple-range random walk algorithm to calculate the density of states. Phys Rev Lett 86:2050–2053
32. Wang F, Landau DP (2001) Determining the density of states for classical statistical models: a random walk algorithm to produce a flat histogram. Phys Rev E 64:056101
33. Yan Q, Faller R, de Pablo JJ (2002) Density-of-states Monte Carlo method for simulation of fluids. J Chem Phys 116:8745–8749
34. Laio A, Parrinello M (2002) Escaping free-energy minima. Proc Natl Acad Sci USA 99:12562–12566
35. Trebst S, Huse DA, Troyer M (2004) Optimizing the ensemble for equilibration in broad-histogram Monte Carlo simulations. Phys Rev E 70:046701
36. Berg BA, Celik T (1992) New approach to spin-glass simulations. Phys Rev Lett 69:2292–2295
37. Berg BA, Hansmann UHE, Neuhaus T (1993) Simulation of an ensemble with varying magnetic field: a numerical determination of the order-order interface tension in the D=2 Ising model. Phys Rev B 47:497–500
38. Janke W, Kappler S (1995) Phys Rev Lett 74:212–215
39. Berg BA, Janke W (1998) Phys Rev Lett 80:4771–4774
40. Hatano N, Gubernatis JE (2000) A multicanonical Monte Carlo study of the 3D +/- J spin glass. Prog Theor Phys (Suppl) 138:442–447
41. Berg BA, Billoire A, Janke W (2000) Spin-glass overlap barriers in three and four dimensions. Phys Rev B 61:12143–12150
42. Berg BA, Muguruma C, Okamoto Y (2007) Residual entropy of ordinary ice from multicanonical simulations. Phys Rev B 75:092202

43. Hansmann UHE, Okamoto Y (1993) Prediction of peptide conformation by multicanonical algorithm—new approach to the multiple-minima problem. J Comput Chem 14:1333–1338
44. Hansmann UHE, Okamoto Y (1994) Comparative study of multicanonical and simulated annealing algorithms in the protein folding problem. Physica A 212:415–437
45. Okamoto Y, Hansmann UHE (1995) Thermodynamics of helix-coil transitions studied by multicanonical algorithms. J Phys Chem 99:11276–11287
46. Wilding NB (1995) Critical-point and coexistence-curve properties of the Lennard–-Jones fluid: a finite-size scaling study. Phys Rev E 52:602–611
47. Kolinski A, Galazka W, Skolnick J (1996) On the origin of the cooperativity of protein folding: implications from model simulations. Proteins 26:271–287
48. Urakami N, Takasu M (1996) Multicanonical Monte Carlo simulation of a polymer with stickers. J Phys Soc Jpn 65:2694–2699
49. Kumar S, Payne P, Vásquez M (1996) Method for free-energy calculations using iterative techniques. J Comput Chem 17:1269–1275
50. Hansmann UHE, Okamoto Y, Eisenmenger F (1996) Molecular dynamics, Langevin and hybrid Monte Carlo simulations in a multicanonical ensemble. Chem Phys Lett 259:321–330
51. Hansmann UHE, Okamoto Y (1996) Monte Carlo simulations in generalized ensemble: multicanonical algorithm versus simulated tempering. Phys Rev E 54:5863–5865
52. Hansmann UHE, Okamoto Y (1997) Numerical comparisons of three recently proposed algorithms in the protein folding problem. J Comput Chem 18:920–933
53. Noguchi H, Yoshikawa K (1997) First-order phase transition in a stiff polymer chain. Chem Phys Lett 278:184–188
54. Nakajima N, Nakamura H, Kidera A (1997) Multicanonical ensemble generated by molecular dynamics simulation for enhanced conformational sampling of peptides. J Phys Chem B 101:817–824
55. Bartels C, Karplus M (1997) Multidimensional adaptive umbrella sampling: applications to main chain and side chain peptide conformations. J Comput Chem 18:1450–1462
56. Higo J, Nakajima N, Shirai H, Kidera A, Nakamura H (1997) Two-component multicanonical Monte Carlo method for effective conformation sampling. J Comput Chem 18:2086–2092
57. Iba Y, Chikenji G, Kikuchi M (1998) Simulation of lattice polymers with multi-self-overlap ensemble. J Phys Soc Jpn 67:3327–3330
58. Mitsutake A, Hansmann UHE, Okamoto Y (1998) Temperature dependence of distributions of conformations of a small peptide. J Mol Graphics Mod 16:226–238; 262–263
59. Hansmann UHE, Okamoto Y (1999) Effects of side-chain charges on alpha-helix stability in C-peptide of ribonuclease A studied by multicanonical algorithm. J Phys Chem B 103:1595–1604
60. Shimizu H, Uehara K, Yamamoto K, Hiwatari Y (1999) Structural phase transition of di-block polyampholyte. Mol Sim 22:285–301
61. Ono S, Nakajima N, Higo J, Nakamura H (1999) The multicanonical weighted histogram analysis method for the free-energy landscape along structural transition paths. Chem Phys Lett 312:247–254
62. Mitsutake A, Okamoto Y (2000) Helix-coil transitions of amino-acid homo-oligomers in aqueous solution studied by multicanonical simulations. J Chem Phys 112:10638–10647
63. Sayano K, Kono H, Gromiha MM, Sarai A (2000) Multicanonical Monte Carlo calculation of the free-energy map of the base-amino acid interaction. J Comput Chem 21:954–962
64. Yasar F, Celik T, Berg BA, Meirovitch H (2000) Multicanonical procedure for continuum peptide models. J Comput Chem 21:1251–1261
65. Mitsutake A, Kinoshita M, Okamoto Y, Hirata F (2000) Multicanonical algorithm combined with the RISM theory for simulating peptides in aqueous solution. Chem Phys Lett 329:295–303
66. Cheung MS, Garcia AE, Onuchic JN (2002) Protein folding mediated by solvation: water expulsion and formation of the hydrophobic core occur after the structural collapse. Proc Natl Acad Sci USA 99:685–690
67. Kamiya N, Higo J, Nakamura H (2002) Conformational transition states of a beta-hairpin peptide between the ordered and disordered conformations in explicit water. Protein Sci 11:2297–2307
68. Jang SM, Pak Y, Shin SM (2002) Multicanonical ensemble with Nose–Hoover molecular dynamics simulation. J Chem Phys 116:4782–4786
69. Terada T, Matsuo Y, Kidera A (2003) A method for evaluating multicanonical potential function without iterative refinement: application to conformational sampling of a

globular protein in water. J Chem Phys 118:4306–4311
70. Berg BA, Noguchi H, Okamoto Y (2003) Multioverlap simulations for transitions between reference configurations. Phys Rev E 68:036126
71. Bachmann M, Janke W (2003) Multicanonical chain-growth algorithm. Phys Rev Lett 91:208105
72. Okumura H, Okamoto Y (2004) Monte Carlo simulations in multibaric-multithermal ensemble. Chem Phys Lett 383:391–396
73. Okumura H, Okamoto Y (2004) Monte Carlo simulations in generalized isobaric-isothermal ensembles. Phys Rev E 70:026702
74. Okumura H, Okamoto Y (2004) Molecular dynamics simulations in the multibaric-multithermal ensemble. Chem Phys Lett 391:248–253
75. Okumura H, Okamoto Y (2006) Multibaric-multithermal ensemble molecular dynamics simulations. J Comput Chem 27:379–395
76. Itoh SG, Okamoto Y (2004) Multi-overlap molecular dynamics methods for biomolecular systems. Chem Phys Lett 400:308–313
77. Sugita Y, Okamoto Y (2005) Molecular mechanism for stabilizing a short helical peptide studied by generalized-ensemble simulations with explicit solvent. Biophys J 88:3180–3190
78. Itoh SG, Okamoto Y (2007) Effective sampling in the configurational space of a small peptide by the multicanonical-multioverlap algorithm. Phys Rev E 76:026705
79. Munakata T, Oyama S (1996) Adaptation and linear-response theory. Phys Rev E 54:4394–4398
80. Lyubartsev AP, Martinovski AA, Shevkunov SV, Vorontsov-Velyaminov PN (1992) New approach to Monte Carlo calculation of the free energy—method of expanded ensemble. J Chem Phys 96:1776–1783
81. Marinari E, Parisi G (1992) Simulated tempering—a new Monte Carlo scheme. Europhys Lett 19:451–458
82. Marinari E, Parisi G, Ruiz-Lorenzo JJ (1997) Numerical simulations of spin glass systems. In: Young AP (ed) Spin glasses and random fields. World Scientific, Singapore, pp 59–98
83. Escobedo FA, de Pablo JJ (1995) Monte Carlo simulation of the chemical potential of polymers in an expanded ensemble. J Chem Phys 103:2703–2710
84. Irbäck A, Potthast F (1995) Studies of an off-lattice model for protein folding—sequence dependence and improved sampling at finite temperature. J Chem Phys 103:10298–10305
85. Irbäck A, Sandelin E (1999) Monte Carlo study of the phase structure of compact polymer chains. J Chem Phys 110:12256–12262
86. Mitsutake A, Okamoto Y (2000) Replica-exchange simulated tempering method for simulations of frustrated systems. Chem Phys Lett 332:131–138
87. Mitsutake A, Okamoto Y (2004) Replica-exchange extensions of simulated tempering method. J Chem Phys 121:2491–2504
88. Park S, Pande V (2007) Choosing weights for simulated tempering. Phys Rev E 76:016703
89. Zheng L, Chen M, Yang W (2009) Simultaneous escaping of explicit and hidden free energy barriers: application of the orthogonal space random walk strategy in generalized ensemble based conformational sampling. J Chem Phys 130:234105
90. Zhang C, Ma J (2010) Enhanced sampling and applications in protein folding in explicit solvent. J Chem Phys 132:244101
91. Kim J, Straub JE (2010) Generalized simulated tempering for exploring strong phase transitions. J Chem Phys 133:154101
92. Hukushima K, Nemoto K (1996) Exchange Monte Carlo method and application to spin glass simulations. J Phys Soc Jpn 65:1604–1608
93. Hukushima K, Takayama H, Nemoto K (1996) Application of an extended ensemble method to spin glasses. Int J Mod Phys C 7:337–344
94. Geyer CJ (1991) Markov chain Monte Carlo maximum likelihood. In: Keramidas EM (ed) Computing science and statistics: proceedings 23rd symposium on the interface. Interface Foundation, Fairfax Station, pp 156–163
95. Swendsen RH, Wang J-S (1986) Replica Monte Carlo simulation of spin glasses. Phys Rev Lett 57:2607–2609
96. Kimura K, Taki K (1991) Time-homogeneous parallel annealing algorithm. In: Vichnevetsky R, Miller, JJH (eds) IMACS 91 Proceedings of the 13th World Congress on Computation and Applied Mathematics, vol 2. pp 827–828
97. Frantz DD, Freeman DL, Doll JD (1990) Reducing quasi-ergodic behavior in Monte Carlo simulations by J-walking—applications to atomic clusters. J Chem Phys 93:2769–2784
98. Tesi MC, van Rensburg EJJ, Orlandini E, Whittington SG (1996) Monte Carlo study of the interacting self-avoiding walk model in three dimensions. J Stat Phys 82:155–181

99. Iba Y (2001) Extended ensemble Monte Carlo. Int J Mod Phys C 12:623–656
100. Hansmann UHE (1997) Parallel tempering algorithm for conformational studies of biological molecules. Chem Phys Lett 281:140–150
101. Sugita Y, Okamoto Y (1999) Replica-exchange molecular dynamics method for protein folding. Chem Phys Lett 314:141–151
102. Wu MG, Deem MW (1999) Efficient Monte Carlo methods for cyclic peptides. Mol Phys 97:559–580
103. Sugita Y, Kitao A, Okamoto Y (2000) Multidimensional replica-exchange method for free-energy calculations. J Chem Phys 113:6042–6051
104. Woods CJ, Essex JW, King MA (2003) The development of replica-exchange-based free-energy methods. J Phys Chem B 107:13703–13710
105. Sugita Y, Okamoto Y (2000) Replica-exchange multicanonical algorithm and multicanonical replica-exchange method for simulating systems with rough energy landscape. Chem Phys Lett 329:261–270
106. Gront D, Kolinski A, Skolnick J (2000) Comparison of three Monte Carlo conformational search strategies for a proteinlike homopolymer model: folding thermodynamics and identification of low-energy structures. J Chem Phys 113:5065–5071
107. Verkhivker GM, Rejto PA, Bouzida D, Arthurs S,Colson AB, Freer ST, Gehlhaar DK, Larson V, Luty BA, Marrone T, Rose PW (2001) Parallel simulated tempering dynamics of ligand-protein binding with ensembles of protein conformations. Chem Phys Lett 337:181–189
108. Fukunishi F, Watanabe O, Takada S (2002) On the Hamiltonian replica exchange method for efficient sampling of biomolecular systems: application to protein structure prediction. J Chem Phys 116:9058–9067
109. Mitsutake A, Sugita Y, Okamoto Y (2003) Replica-exchange multicanonical and multicanonical replica-exchange Monte Carlo simulations of peptides. I. Formulation and benchmark test. J Chem Phys 118:6664–6675
110. Mitsutake A, Sugita Y, Okamoto Y (2003) Replica-exchange multicanonical and multicanonical replica-exchange Monte Carlo simulations of peptides. II. Application to a more complex system. J Chem Phys 118:6676–6688
111. Sikorski A, Romiszowski P (2003) Thermodynamical properties of simple models of protein-like heteropolymers. Biopolymers 69:391–398
112. Lin CY, Hu CK, Hansmann UHE (2003) Parallel tempering simulations of HP-36. Proteins 52:436–445
113. La Penna G, Mitsutake A, Masuya M, Okamoto Y (2003) Molecular dynamics of C-peptide of ribonuclease A studied by replica-exchange Monte Carlo method and diffusion theory. Chem Phys Lett 380:609–619
114. Kokubo H, Okamoto Y (2004) Prediction of membrane protein structures by replica-exchange Monte Carlo simulations: case of two helices. J Chem Phys 120:10837
115. Kokubo H, Okamoto Y (2009) Analysis of helix-helix interactions of bacteriorhodopsin by replica-exhcange simulations. Biophys J 96:765–776
116. Falcioni M, Deem DW (1999) A biased Monte Carlo scheme for zeolite structure solution. J Chem Phys 110:1754–1766
117. Yan Q, de Pablo JJ (1999) Hyper-parallel tempering Monte Carlo: application to the Lennard–Jones fluid and the restricted primitive model. J Chem Phys 111:9509–9516
118. Nishikawa T, Ohtsuka H, Sugita Y, Mikami M, Okamoto Y (2000) Replica-exchange Monte Carlo method for Ar fluid. Prog Theor Phys (Suppl) 138:270–271
119. Kofke DA (2002) On the acceptance probability of replica-exchange Monte Carlo trials. J Chem Phys 117:6911–6914
120. Okabe T, Kawata M, Okamoto Y, Mikami M (2001) Replica-exchange Monte Carlo method for the isobaric-isothermal ensemble. Chem Phys Lett 335:435–439
121. Ishikawa Y, Sugita Y, Nishikawa T, Okamoto Y (2001) Ab initio replica-exchange Monte Carlo method for cluster studies. Chem Phys Lett 333:199–206
122. Garcia AE, Sanbonmatsu KY (2001) Exploring the energy landscape of a beta hairpin in explicit solvent. Proteins 42:345–354
123. Zhou RH, Berne BJ, Germain R (2001) The free energy landscape for beta hairpin folding in explicit water. Proc Natl Acad Sci USA 98:14931–14936
124. Garcia AE, Sanbonmatsu KY (2002) α-Helical stabilization by side chain shielding of backbone hydrogen bonds. Proc Natl Acad Sci USA 99:2782–2787
125. Zhou RH, Berne BJ (2002) Proc Natl Acad Sci USA 99:12777–12782

126. Feig M, MacKerell AD, Brooks CL III (2003) Force field influence on the observation of pi-helical protein structures in molecular dynamics simulations. J Phys Chem B 107:2831–2836
127. Rhee YM, Pande VS (2003) Multiplexed-replica exchange molecular dynamics method for protein folding simulation. Biophys J 84:775–786
128. Paschek D, Garcia AE (2004) Reversible temperature and pressure denaturation of a protein fragment: a replica exchange molecular dynamics simulation study. Phys Rev Lett 93:238105
129. Paschek D, Gnanakaran S, Garcia AE (2005) Simulations of the pressure and temperature unfolding of an α-helical peptide. Proc Natl Acad Sci USA 102:6765–6770
130. Pitera JW, Swope W (2003) Understanding folding and design: replica-exchange simulations of "Trp-cage" fly miniproteins. Proc Natl Acad Sci USA 100:7587–7592
131. Ohkubo YZ, Brooks CL III (2003) Exploring Flory's isolated-pair hypothesis: Statistical mechanics of helix-coil transitions in polyalanine and the C-peptide from RNase A. Proc Natl Acad Sci USA 100:13916–13921
132. Fenwick MK, Escobedo FA (2003) Hybrid Monte Carlo with multidimensional replica exchanges: conformational equilibria of the hypervariable reigons of a llamma V-HH antibody domain. Biopolymers 68:160–177
133. Xu HF, Berne BJ (2000) Multicanonical jump walking annealing: an efficient method for geometric optimization. J Chem Phys 112:2701–2708
134. Faller R, Yan Q, de Pablo JJ (2002) Multicanonical parallel tempering. J Chem Phys 116:5419–5423
135. Fenwick MK, Escobedo FA (2003) Expanded ensemble and replica exchange methods for simulation of protein-like systems. J Chem Phys 119:11998–12010
136. Murata K, Sugita Y, Okamoto Y (2004) Free energy calculations for DNA base stacking by replica-exchange umbrella sampling. Chem Phys Lett 385:1–7
137. Felts AK, Harano Y, Gallicchio E, Levy RM (2004) Free energy surfaces of β-hairpin and α-helical peptides generated by replica exchange molecular dynamics with the AGBNP implicit solvent model. Proteins 56:310–321
138. Mitsutake A, Kinoshita M, Okamoto Y, Hirata F (2004) Combination of the replica-exchange Monte Carlo method and the reference interaction site model theory for simulating a peptide molecule in aqueous solution. J Phys Chem B 108:19002–19012
139. Baumketner A, Shea JE (2005) Free energy landscapes for amyloidogenic tetrapeptides dimerization. Biophys J 89:1493–1503
140. Yoda T, Sugita Y, Okamoto Y (2007) Cooperative folding mechanism of a beta-hairpin peptide studied by a multicanonical replica-exchange molecular dynamics simulation. Proteins 66:846–859
141. Roitberg AE, Okur A, Simmerling C (2007) Coupling of replica exchange simulations to a non-Boltzmann structure reservoir. J Phys Chem B 111:2415–2418
142. Rosta E, Buchete N-Y, Hummber G (2009) Thermostat artifacts in replica exchange molecular dynamics simulations. J Chem Theory Comput 5:1393–1399
143. Yoda T, Sugita Y, Okamoto Y (2010) Hydrophobic core formation and dehydration in protein folding studied by generalized-ensemble simulations. Biophys J 99:1637–1644
144. De Simone A, Derreumaux P (2010) Low molecular weight oligomers of amyloid peptides display β-barrel conformations: a replica exchange molecular dynamics study in explicit solvent. J Chem Phys 132:165103
145. Hukushima K (1999) Domain-wall free energy of spin-glass models: numerical method and boundary conditions. Phys Rev E 60:3606–3614
146. Whitfield TW, Bu L, Straub JE (2002) Generalized parallel sampling. Physica A 305:157–171
147. Kwak W, Hansmann UHE (2005) Efficient sampling of protein structures by model hopping. Phys Rev Lett 95:138102
148. Bunker A, Dünweg B (2000) Parallel excluded volume tempering for polymer melts. Phys Rev E 63:016701
149. Liu P, Kim B, Friesner RA, Bern BJ (2005) Replica exchange with solute tempering: a method for sampling biological systems in explicit water. Proc Natl Acad Sci USA 102:13749–13754
150. Affentranger R, Tavernelli I, Di Iorio EE (2006) A novel Hamiltonian replica exchange MD protocol to enhance protein conformational space sampling. J Chem Theory Comput 2:217–228
151. Lou H, Cukier RI (2006) Molecular dynamics of apo-adenylate kinase: a distance replica exchange method for the free energy of conformational fluctuations. J Phys Chem B 110:24121–24137

152. Mu Y (2009) Dissociation aided and side chain sampling enhanced Hamiltonian replica exchange. J Chem Phys 130:164107
153. Itoh SG, Okumura H, Okamoto Y (2010) Replica-exchange method in van der Waals radius space: overcoming steric restrictions for biomolecules. J Chem Phys 132:134105
154. Mitsutake A, Okamoto Y (2009) From multidimensional replica-exchange method to multidimensional multicanonical algorithm and simulated tempering. Phys Rev E 79:047701
155. Mitsutake A, Okamoto Y (2009) Multidimensional generalized-ensemble algorithms for complex systems. J Chem Phys 130:214105
156. Mitsutake A (2009) Simulated-tempering replica-exchange method for the multidimensional version. J Chem Phys 131:094105
157. Mori Y, Okamoto Y (2010) Generalized-ensemble algorithms for the isobaric-isothermal ensemble. J Phys Soc Jpn 79:074003
158. Metropolis N, Rosenbluth AW, Rosenbluth MN, Teller AH, Teller E (1953) Equation of state calculations by fast computing machines. J Chem Phys 21:1087–1092
159. Nosé S (1984) A molecular dynamics method for simulations in the canonical ensemble. Mol Phys 52:255–268
160. Nosé S (1984) A unified formulation of the constant temperature molecular dynamics methods. J Chem Phys 81:511–519
161. Shirts MR, Chodera JD (2008) Statistically optimal analysis of samples from multiple equilibrium states. J Chem Phys 129:124105
162. Berg BA (2003) Multicanonical simulations step by step. Comp Phys Commun 153:397–406
163. Mori Y, Okamoto Y (2010) Replica-exchange molecular dynamics simulations for various constant temperature algorithms. J Phys Soc Jpn 79:074001
164. Allen MP, Tildesley DJ (1987) Computer Simulation of Liquids. Oxford, New York, p 259
165. Andersen HG (1980) Molecular dynamics simulations at constant pressure and/or temperature. J Chem Phys 72:2384–2393
166. Hoover WG, Ladd AJC, Moran B (1982) High strain rate plastic flow studied via non-equilibrium molecular dynamics. Phys Rev Lett 48:1818–1820
167. Evans DJ (1983) Computer experiment for non-linear thermodynamics of couette flow. J Chem Phys 78:3297–3302
168. Evans DJ, Morriss GP (1983) The isothermal isobaric molecular dynamics ensemble. Phys Lett A 98:433–436
169. Hoover WG (1985) Canonical dynamics—equilibrium phase space distributions. Phys Rev A 31:1695–1697
170. Martyna GJ, Klein ML, Tuckerman M (1992) Nosé–Hoover chains—the canonical ensemble via continuous dynamics. J Chem Phys 97:2635–2643
171. Bond SD, Leimkuhler BJ, Laird BB (1999) The Nosé–Poincaré method for constant temperature molecular dynamics. J Comput Phys 151:114–134
172. McDonald IR (1972) NpT-ensemble Monte Carlo calculations for binary liquid mixtures. Mol Phys 23:41-58
173. Myers JK, Pace CN, Scholtz JM (1997) A direct comparison of helix propensity in proteins and peptides. Proc Natl Acad Sci USA 94:2833–2837
174. Momany FA, McGuire RF, Burgess AW, Scheraga HA (1975) Energy parameters in polypeptides. VII. Geometric parameters, partial atomic charges, nonbonded interactions, hydrogen bond interactions, and intrinsic torsional potentials for the naturally occurring amino acids. J Phys Chem 79:2361–2381
175. Némethy G, Pottle MS, Scheraga HA (1983) Energy parameters in polypeptides. 9. Updating of geometrical parameters, nonbonded interactions, and hydrogen bond interactions for the naturally occurring amino acids. J Phys Chem 87:1883–1887
176. Sippl MJ, Némethy G, Scheraga HA (1984) Intermolecular potentials from crystal data. 6. Determination of empirical potentials for O-H...O=C hydrogen bonds from packing configurations. J Phys Chem 88:6231–6233
177. Ooi T, Oobatake M, Némethy G, Scheraga HA (1987) Accessible surface areas as a measure of the thermodynamic parameters of hydration of peptides. Proc Natl Acad Sci USA 84:3086–3090
178. Masuya M, unpublished; see http://biocomputing.cc/nsol/.
179. Kitahara R, Akasaka K (2003) Close identity of a pressure-stabilized intermediate with a kinetic intermediate in protein folding. Proc Natl Acad Sci USA 100:3167–3172
180. Kitahara R, Yokoyama S, Akasaka K (2005) NMR snapshots of a fluctuating protein structure: ubiquitin at 30 bar–3 kbar. J Mol Biol 347:277–285

181. Quigley D, Probert MIJ (2004) Landevin dynamics in constant pressure extended systems. J Chem Phys 120:11432–11441
182. Darden T, York D, Pedersen L (1993) Particle mesh Ewald—an Nlog(N) method for Ewald sums in large systems. J Chem Phys 98:10089–10092
183. Essmann U, Perera L, Berkowitz ML, Darden T, Lee H, Pedersen LG (1995) A smooth particle mesh Ewald method. J Chem Phys 103:8577–8593
184. MacKerell AD Jr, Bashford D, Bellott M, Dunbrack RL Jr, Evanseck JD, Field MJ, Fischer S, Gao J, Guo H, Ha S, Joseph-McCarthy D, Kuchnir L, Kuczera K, Lau FTK, Mattos C, Michnick S, Ngo T, Nguyen DT, Prodhom B, Reiher WE III, Roux B, Schlenkrich M, Smith JC, Stote R, Straub J, Watanabe M, Wiórkiewicz-Kuczera J, Yin D, Karplus M (1998) All-atom empirical potential for molecular modeling and dynamics studies of proteins. J Phys Chem B 102:3586–3616
185. MacKerell AD Jr, Feig M, Brooks CL III (2004) Improved treatment of the protein backbone in empirical force fields. J Am Chem Soc 126:698–699
186. MacKerell AD Jr, Feig M, Brooks CL III (2004) Extending the treatment of backbone energetics in protein force fields: Limitations of gas-phase quantum mechanics in reproducing protein conformational distributions in molecular dynamics simulations. J Comput Chem 25:1400–1415
187. Jorgensen WL, Chandrasekhar J, Madura JD, Impey RW, Klein ML (1983) Comparison of simple potential functions for simulating liquid water. J Chem Phys 79:926–935
188. Phillips JC, Braun R, Wang W, Gumbart J, Tajkhorshid E, Villa E, Chipot C, Skeel RD, Kale L, Schulten K (2005) Scalable molecular dynamics with NAMD. J Comput Chem 26:1781–1802